Electrophoresis and Western blotting

Sodium dodecyl sulphate-polyacrylamide gel electrophoresis (SDS–PAGE) was performed using 8% and 13% gels at 150 V for 1 h in a Bio-Rad mini-gel apparatus, followed by silver staining. For Western blotting, the protein was transferred to a polyvinylidene difluoride membrane and probed using the indicated mAbs, followed by anti-mouse peroxidase-conjugated secondary antibody (Stressgen Bioreagents, Ann Arbor, MI, USA). Signals were detected using enhanced chemiluminescence (PerkinElmer Life Science, Boston, MA, USA).

Results

Immunoblot analysis of resin-treated FVIII

We have reported that the iminodiacetate resin resulted in the complete loss of FVIII activity by direct deprivation of predominant Ca^{2+} ($>Mn^{2+}>>Cu^{2+}$) and VWF protected FVIII antigen from resin-induced degradation (Takeyama *et al*, 2008). We speculated that the resin induced significant disturbances in antigenicity and/or structure of FVIII and that VWF prevented such significant changes. To confirm this, SDS-PAGE and Western blotting analyses of resin-treated FVIII were performed in the absence or presence of VWF (Fig 1). Analysis by silver staining showed that the pattern of SDS–PAGE on resin-treated FVIII was similar to that on untreated FVIII, representing the presence of treated FVIII protein in eluted sample and non-precipitation (Fig 1A). In Western blot, the HCh was visualized using anti-A1 and anti-

A2 mAbs and the LCh was visualized using anti-A3 and anti-C2 mAbs. Multi-sized HCh fragments with molecular mass of 90~210 kDa were preserved in resin-treated FVIII alone. This pattern was similar to that using untreated FVIII (Fig 1B, C). Similarly, HCh fragments with higher molecular sizes were also evident in the treated FVIII/VWF complex, indicating that the structure of the HCh was not affected by resin treatment. In contrast, the 80-kDa LCh fragment, detected by anti-A3 mAb, was faintly detected in resin-treated FVIII alone compared with untreated FVIII (Fig 1D). The high molecular weight species in the FVIII LCh band were observed in treated FVIII alone, but this origin is unclear at present. Furthermore, no bands were visible using an anti-C2 mAb (Fig 1E). However, with the treated FVIII/VWF complex, the 80-kDa LCh fragment was detected using both mAbs, although the reactivity with the anti-C2 mAb was weaker than that with untreated FVIII. AS FVIII dissociates from VWF by thrombin cleavage, Western blot for resin-treated thrombin-cleaved FVIII/VWF was performed using an anti-C2 mAb. No bands in the treated cleaved FVIII/VWF complex were visible, similar to resin-treated FVIII alone (data not shown), supporting that free FVIII(a) could not be protected from the resin-induced structural impairment. These results suggested that the antigenic structure of the LCh, especially the C2 domain, was affected more predominantly than the A3 domain by treatment with the resin, and that complex formation with VWF protected FVIII from the resin-induced structural impairment of the LCh.

The possibility that the LCh in treated FVIII was not bound adequately to the polyvinylidene difluoride transfer-membrane, because of the impaired structure of the fragment, was
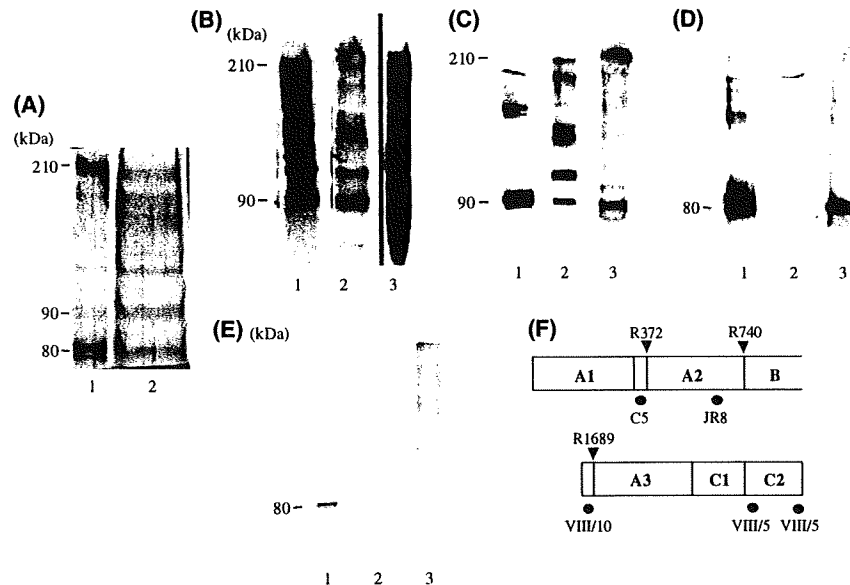

Fig 1. Western blotting for FVIII and FVIII/VWF complex treated by the iminodiacetate resin. Equivalent amounts (0·6 μg) of FVIII (*lane 1*), treated FVIII (*lane 2*), and treated FVIII/VWF complex (*lane 3*) were run on 8% gels prior to the silver staining (A), and prior to Western blotting using anti-A1 (C5, B), anti-A2 (JR8, C), anti-A3 (NMC-VIII/10, D), and anti-C2 (NMC-VIII/5, E) monoclonal antibodies (mAbs). *Panel* F shows a schematic presentation of the domain organization of the HCh, LCh, and epitope regions of mAbs.
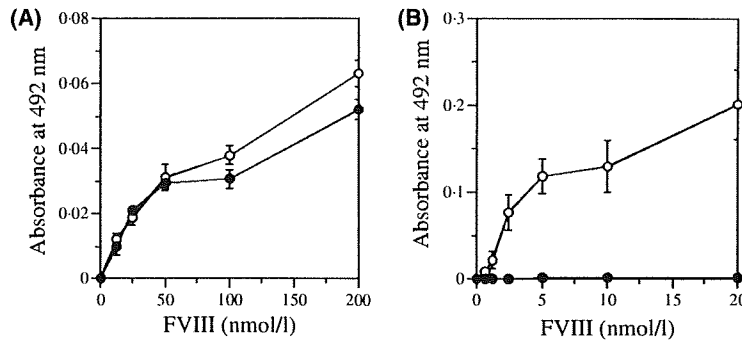
Fig 2. ELISA for FVIII and resin-treated FVIII using anti-A2 or anti-C2 antibody. Various amounts of FVIII (*open circles*) and iminodiacetate resin-treated FVIII (*closed circles*) were reacted with anti-A2 mAb (JR8, A) or anti-C2 polyclonal antibody (B) that had been immobilized onto microtitre wells for 2 h. Bound FVIII was detected using biotinylated anti-A2 mAb (R8B12) and anti-C2 antibody, respectively. Absorbance values were plotted as a function of the concentration of FVIII. Data represent the average values and standard deviations obtained from at least three separate experiments.

excluded by visualizing the LCh fragments using Ponceau S (data not shown). Furthermore, sandwich ELISAs for detection of the HCh and LCh also showed that the A2 domain of the HCh in resin-treated FVIII was present in equivalent concentrations to those observed in untreated FVIII (Fig 2A). However, the C2 domain of the LCh was not detected in treated FVIII (Fig 2B). These results again indicated that severe impairment of the C2 domain structure by the resin resulted in the loss of reactivity with the anti-C2 antibody, consistent with those of immunoblot analysis.

Effects of VWF on the resin treatment of the C2 domain

The observations that the iminodiacetate resin disturbed the FVIII C2 structure and that VWF protected FVIII from the resin-induced reaction, prompted an extension of the experiments using recombinant C2 domain. Recombinant C2 preparations (1 μmol/l), in the absence or presence of

equivalent molar concentrations of VWF, were treated with 10% (w/v) iminodiacetate resin. Samples were run on 13% gels, followed by silver staining and by Western blotting using an anti-C2 mAb (NMC-VIII/5) (Fig 3). The patterns of SDS-PAGE on resin-treated C2 (*lane 2*) as well as EDTA-treated C2 (*lane 3*) were similar to that on untreated C2 (*lane 1*), also supporting the presence of treated C2 protein in eluted sample and non-precipitation (*panel A*). Under these conditions, more than 90% C2 should be present as the C2/VWF complex, since the C2 domain binds to VWF with weak affinity (K_d: *c*.500 nmol/l) (Saenko & Scandella, 1997). In control experiments, untreated FVIII (*lane 1*), C2 alone (*lane 2*), and C2/VWF complex (*lane 3*) showed similar reactivities with anti-C2 mAb (*panel B*). The reactivity was completely lost in resin-treated C2 alone (*lane 4*). However, reactivity was preserved in the resin-treated C2/VWF complex (*lane 5*), consistent with the data obtained in the above experiments using FVIII. Interestingly, the well-known metal ion-chelator, EDTA, did
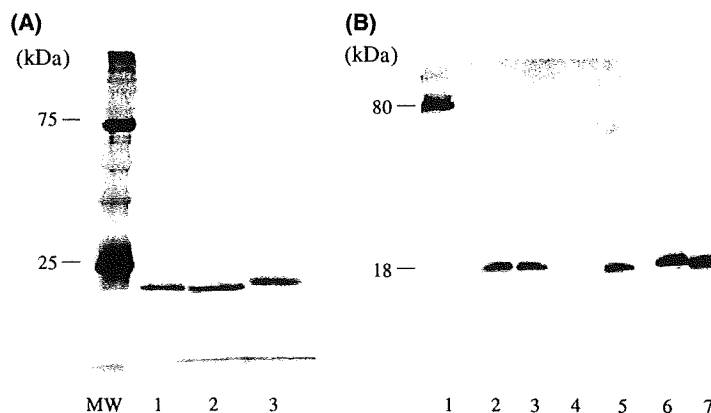

Fig 3. Effect of VWF on the resin-induced reaction with the C2 domain. Recombinant C2 (500 nmol/l), in the absence or presence of equivalent molar concentrations of VWF, was treated with 10% (w/v) iminodiacetate resin or 10 mmol/l EDTA. Samples were run on 13% gels prior to the silver staining (A) and prior to Western blotting (B) using an anti-C2 mAb (NMC-VIII/5). (*Panel* A) Lanes 1–3 show the untreated C2 alone, resin-treated C2, and EDTA-treated C2, respectively. (*Panel* B) Lane 1 shows untreated FVIII. Lanes 2–7 show the C2 alone, C2/VWF complex, resins-treated C2, resins-treated C2/VWF, EDTA-treated C2 alone and EDTA-treated C2/VWF, respectively.

not affect the reactivity of the C2 and C2/VWF with the anti-C2 mAb (lanes 6 and 7, respectively). These findings provided further evidence that the resin impaired the structure of the C2 domain, and that this was moderated by VWF.

Interactions of resin-treated FVIII (or C2) with VWF or phospholipid

We further investigated whether resin-treated FVIII or C2 domain retained the binding ability for VWF by kinetic measurements using SPR-based assays. Fig 4 shows the representative data of association curves of FVIII (Fig 4A) and C2 (Fig 4B) to immobilized VWF. Untreated FVIII bound to VWF (K_d; c. 1 nmol/l) in a dose-dependent manner, consistent with previous reports (Saenko & Scandella, 1997), whilst the treated FVIII failed to interact. Similar results at lower affinity were obtained using C2 domain. Untreated C2 domain bound to immobilized VWF (K_d; c. 500 nmol/l), but not the resin-treated C2.

Given that the FVIII C2 domain contains a major phospholipid-interactive site(s) (Foster et al, 1990), further experiments were performed to assess the effect of resin-treatment on phospholipid binding. The phospholipid binding affinity (K_d) for FVIII was c. 1 nmol/l, whilst the treated FVIII and the treated C2 domain little interacted with phospholipid (data not shown). These results also supported that iminodiacetate resin disrupted the normal structure of the C2 domain.

Deprivation of Ca^{2+} in recombinant C2 by iminodiacetate resin

Our recent report (Takeyama et al, 2008) demonstrated that the concentration of Ca^{2+} involved in recombinant FVIII was decreased by >95% with the resin treatment. Similarly, the effect of this resin on the concentration of Ca^{2+} in recombinant C2 domain was examined. The concentration

of Ca^{2+} in untreated C2 was 0·037 mmol/l, and that in treated C2 was 0·017 mmol/l, showing that the resin deprived Ca^{2+} by ~55%. In the control experiment, treatment by EDTA any little affected the concentration of Ca^{2+} (0·037 mmol/l) in C2, indicating that the resin probably disturbed the antigenic conformational structure of the C2 domain by the deprivation of Ca^{2+}.

Ca^{2+} blocks the resin-induced impairment of the C2 structure

Our earlier experiments using Western blotting indicated that iminodiacetate resin impaired the structure and/or antigenicity of the C2 domain, whilst complex formation with VWF was protective. We examined, therefore, whether Ca^{2+} competitively blocked the resin-induced impairment of the C2 structure. The recombinant C2 preparations (1 μmol/l) were mixed with the increasing amounts of Ca^{2+} for 1 h and then incubated with resin for 4 h prior to Western blotting analysis (Fig 5). The C2 band was visualized using anti-C2 mAb. In the absence of Ca^{2+}, treated C2 completely lost reactivity with the antibody (lane 2). In the presence of increasing amounts of Ca^{2+}, however, the C2 domain was detected in a dose-dependent manner (lanes 3–8). Band densitometry showed that the highest concentration of Ca^{2+} employed (300 mmol/l) competitively blocked resin-induced impairment by c. 70%. These results again indicated that iminodiacetate resin impaired the C2 structure by depleting Ca^{2+}, and that VWF protected the C2 domain.

Discussion

Iminodiacetate resin ($N=(CH_2COO)_2^-$) is classified as a cation-exchange resin. Different from cation-exchange resins with carbonate (COO^-) or sulfonate (SO_3^-) groups, the cofactor activity of FVIII was completely lost by treatment with iminodiacetate resin, due to direct deprivation of metal ions,
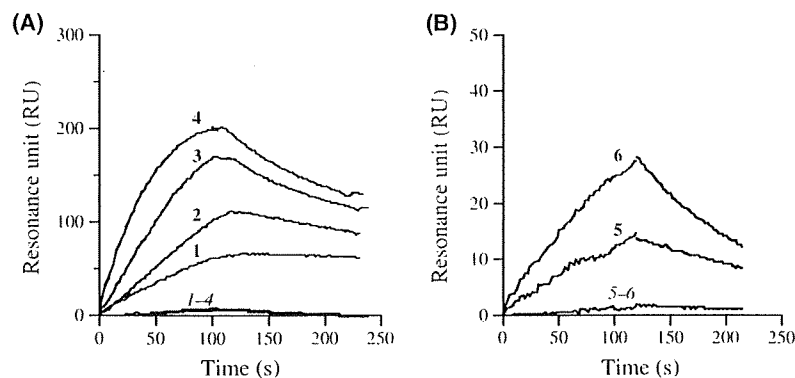

Fig 4. Effect of resin on VWF binding to FVIII or the C2 domain in SPR-based assays. FVIII (A) and recombinant C2 (B) that were untreated (curves 1–6) or treated (curves 1–4 and 5–6) with the iminodiacetate resin were added to VWF immobilized onto the sensor chip. Binding (association) of the ligands was monitored at a flow rate of 10 μl/min for 2 min, and dissociation was monitored for 2 min. The numbers, 1–6, represent concentrations of 5, 10, 20 and 40 nmol/l of FVIII, and 500 and 1000 nmol/l of C2, respectively.
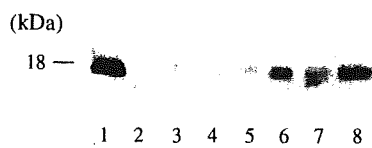
(kDa)

18 —

1 2 3 4 5 6 7 8

Fig 5. Inhibition of resin-induced C2 structural impairment by the addition of Ca^{2+}. A constant concentration (1 μmol/l) of recombinant C2 was mixed with various amounts of Ca^{2+} for 1 h and incubated with the iminodiacetate resin for 4 h prior to Western blotting analysis. The C2 band was visualized using anti-C2 mAb (NMC-VIII/5). *Lane 1* shows untreated C2 alone. *Lanes 2–8* show the treated C2 with Ca^{2+} at 0, 10, 25, 50, 75, 100 and 300 mmol/l, respectively.

predominantly Ca^{2+} (Takeyama *et al*, 2008). Furthermore, the presence of VWF prevented FVIII molecules from resin-induced degradation. It is well known that EDTA also inactivates FVIII by chelating metal ions, due to promoting dissociation of the HCh and LCh (Fay, 1988). Reactivity of the EDTA-separated chains with anti-FVIII mAbs is retained to some extent, however, and FVIII activity can be reconstituted from the isolated both chains by the addition of metal ions. In the present study, therefore, the reactivity of resin-treated FVIII with anti-LCh mAbs (anti-A3 and anti-C2) was abolished, whilst reactivity with anti-HCh mAbs (anti-A1 and anti-A2) was not significantly affected. In particular, treated C2 domain as well as treated FVIII completely failed to react with an anti-C2 mAb. These findings indicated that severe disturbances in conformational structure resulted in the loss of antigenicity of the C2 domain because of deprivation of Ca^{2+}, supporting the different mechanism of EDTA-induced FVIII inactivation.

Western blotting and ELISA demonstrated that iminodiacetate resin caused disturbances in the LCh structure, in particular the C2 domain. In addition, both FVIII and C2 domain treated with resin failed to bind to VWF and phospholipid in SPR-based assays, consistent with changes in the C2 domain structure. These data supported previous reports on the high susceptibility of the C2 domain to structural change. For example, a point-mutation to Cys from Arg at residue 2159 within the marginal region of the C1-C2 domain was shown to markedly reduce C2 antigenicity in a moderate haemophilia A patient (Suzuki *et al*, 1997), enrolled in the haemophilia A database. Also, the administration of silica-absorbed and heat-treated FVIII concentrates to patients with haemophilia A increased the incidence of anti-C2 alloAb inhibitors, suggesting that structural changes in the C2 domain results in higher antigenicity (Sawamoto *et al*, 1998). These reports support the concept that the C2 domain is highly vulnerable to conformational change, and our present data also indicate that instability of the C2 domain is related to a high dependency of the C2 domain on metal ions. However, the reason that the HCh containing Ca^{2+}-binding sites was unaffected by the resin treatment is unclear at present.

A Ca^{2+}-binding region with high affinity (K_d: *c.* 10 μmol/l) has been identified within segment 110–126 of the A1 domain

of FVIII (Wakabayashi *et al*, 2004). In particular, the acidic residues Glu^{110}, Asp^{116}, Glu^{122}, Asp^{125}, and Asp^{126} appeared likely to contribute to Ca^{2+} coordination. Furthermore, a direct binding method using isothermal titration calorimetry indicated that multiple Ca^{2+} binding sites with low affinity (K_d *c.* 4 mmol/l) were present in the LCh (Wakabayashi *et al*, 2004). More recently, Shen *et al* (2008) has reported the crystal structure of FVIII (Shen *et al*, 2008), and that Ca^{2+} is probably also coordinated by two Asp residues (Asp^{538} and Asp^{542}) in the A2 domain. However, in the present study, the presence of a Ca^{2+}-binding site in the C2 domain is raised by several data. Resin-treated C2 completely failed to bind to VWF and phospholipid. Western blotting demonstrated that treated C2 alone was poorly detected by an anti-C2 mAb, but the treated C2/VWF complex was readily visualized. Ca^{2+} competitively blocked resin-induced impairment of the C2 structure. All data are in keeping with the presence of important Ca^{2+}-binding site(s) in the C2 domain.

Moreover, the ability to generate FVIII activity appears to be related to the Ca^{2+}-dependent conformational structure of the C2 domain. The VWF-protection mechanism might be explained by the Ca^{2+}-binding site in the C2 domain being buried by binding to VWF, and being inaccessible to the resin. It is possible, therefore, that the Ca^{2+}-binding site(s) in the C2 domain may overlap the VWF-binding site, although the possibility of steric hindrance cannot be completely excluded. Interestingly, we have observed that the VWF-binding site in the C2 domain juxtaposes to the common epitopes recognized by anti-C2 antibodies (Shima *et al*, 1995; Nogami *et al*, 1999b). Studies are in progress to determine the contribution of specific residues involved in Ca^{2+}-binding and required to maintain the conformational antigenic structure of the LC in FVIII.

Acknowledgements

References

Connerty, H.V. & Briggs, A.R. (1966) Determination of serum calcium by means of orthocresolphthalein complexone. *American Journal of Clinical Pathology*, **45**, 290–296.

van Dieijen, G., Tans, G., Rosing, J. & Hemker, H.C. (1981) The role of phospholipid and factor VIIIa in the activation of bovine factor X. *The Journal of Biological Chemistry*, **256**, 3433–3442.

Eaton, D., Rodriguez, H. & Vehar, G.A. (1986) Proteolytic processing of human factor VIII. Correlation of specific cleavages by thrombin, factor Xa, and activated protein C with activation and inactivation of factor VIII coagulant activity. *Biochemistry*, **25**, 505–512.

Fay, P.J. (1988) Reconstitution of human factor VIII from isolated subunits. *Archives of Biochemistry and Biophysics*, **262**, 525–531.

536

Fay, P.J., Coumans, J.V. & Walker, F.J. (1991) Von Willebrand factor mediates protection of factor VIII from activated protein C-catalyzed inactivation. *The Journal of Biological Chemistry*, **266**, 2172–2177.

Fòster, P.A., Fulcher, C.A., Houghten, R.A. & Zimmerman, T.S. (1990) Synthetic factor VIII peptides with amino acid sequences contained within the C2 domain of factor VIII inhibit factor VIII binding to phosphatidylserine. *Blood*, **75**, 1999–2004.

Kaufman, R.J., Wasley, L.C., Davies, M.V., Wise, R.J., Israel, D.I. & Dorner, A.J. (1989) Effect of von Willebrand factor coexpression on the synthesis and secretion of factor VIII in Chinese hamster ovary cells. *Molecular and Cellular Biology*, **9**, 1233–1242.

Koedam, J.A., Hamer, R.J., Beeser-Visser, N.H., Bouma, B.N. & Sixma, J.J. (1990) The effect of von Willebrand factor on activation of factor VIII by factor Xa. *European Journal of Biochemistry*, **189**, 229–234.

Lollar, P., Hill-Eubanks, D.C. & Parker, C.G. (1988) Association of the factor VIII light chain with von Willebrand factor. *The Journal of Biological Chemistry*, **263**, 10451–10455.

Mann, K.G., Nesheim, M.E., Church, W.R., Haley, P. & Krishnaswamy, S. (1990) Surface-dependent reactions of the vitamin K-dependent enzyme complexes. *Blood*, **76**, 1–16.

Mimms, L.T., Zampighi, G., Nozaki, Y., Tanford, C. & Reynolds, J.A. (1981) Phospholipid vesicle formation and transmembrane protein incorporation using octyl glucoside. *Biochemistry*, **20**, 833–840. 1–16.

Nogami, K., Shima, M., Hosokawa, K., Suzuki, T., Koide, T., Saenko, E.L., Scandella, D., Shibata, M., Kamisue, S., Tanaka, I. & Yoshioka, A. (1999a) Role of factor VIII C2 domain in factor VIII binding to factor Xa. *The Journal of Biological Chemistry*, **274**, 31000–31007.

Nogami, K., Shima, M., Nakai, H., Tanaka, I., Suzuki, H., Morichika, S., Shibata, M., Saenko, E.L., Scandella, D., Giddings, J.C. & Yoshioka, A. (1999b) Identification of a factor VIII peptide, residues 2315–2330, which neutralizes human factor VIII C2 inhibitor alloantibodies: requirement of Cys2326 and Glu2327 for maximum effect. *British Journal of Haematology*, **107**, 196–203.

Nogami, K., Shima, M., Nishiya, K., Hosokawa, K., Saenko, E.L., Sakurai, Y., Shibata, M., Suzuki, H., Tanaka, I. & Yoshioka, A. (2002) A novel mechanism of factor VIII protection by von Willebrand factor from activated protein C-catalyzed inactivation. *Blood*, **99**, 3993–3998.

Saenko, E.L. & Scandella, D. (1997) The acidic region of the factor VIII light chain and the C2 domain together form the high affinity binding site for von willebrand factor. *The Journal of Biological Chemistry*, **272**, 18007–18014.

Saenko, E.L., Shima, M., Rajalakshmi, K.J. & Scandella, D. (1994) A role for the C2 domain of factor VIII in binding to von Willebrand factor. *The Journal of Biological Chemistry*, **269**, 11601–11605.

Saenko, E.L., Yakhyaev, A.V., Mikhailenko, I., Strickland, D.K. & Sarafanov, A.G. (1999) Role of the low density lipoprotein-related protein receptor in mediation of factor VIII catabolism. *The Journal of Biological Chemistry*, **274**, 37685–37692.

Sawamoto, Y., Prescott, R., Zhong, D., Saenko, E.L., Mauser-Bunschoten, E., Peerlinck, K., van den Berg, M. & Scandella, D. (1998) Dominant C2 domain epitope specificity of inhibitor antibodies elicited by a heat pasteurized product, factor VIII CPS-P, in previously treated hemophilia A patients without inhibitors. *Thrombosis Haemostasis*, **79**, 62–68.

Shen, B.W., Spiegel, P.C., Chang, C.H., Huh, J.W., Lee, J.S., Kim, J., Kim, Y.H. & Stoddard, B.L. (2008) The tertiary structure and domain organization of coagulation factor VIII. *Blood*, **111**, 1240–1247.

Shima, M., Yoshioka, A., Nakajima, M., Nakai, H. & Fukui, H. (1992) A monoclonal antibody (NMC-VIII/10) to factor VIII light chain recognizing Glu1675-Glu1684 inhibits factor VIII binding to endogenous von Willebrand factor in human umbilical vein endothelial cells. *British Journal of Haematology*, **81**, 533–538.

Shima, M., Scandella, D., Yoshioka, A., Nakai, H., Tanaka, I., Kamisue, S., Terada, S. & Fukui, H. (1993) A factor VIII neutralizing monoclonal antibody and a human inhibitor alloantibody recognizing epitopes in the C2 domain inhibit factor VIII binding to von Willebrand factor and to phosphatidylserine. *Thrombosis Haemostasis*, **69**, 240–246.

Shima, M., Nakai, H., Scandella, D., Tanaka, I., Sawamoto, Y., Kamisue, S., Morichika, S., Murakami, T. & Yoshioka, A. (1995) Common inhibitory effects of human anti-C2 domain inhibitor alloantibodies on factor VIII binding to von Willebrand factor. *British Journal of Haematology*, **91**, 714–721.

Suzuki, H., Shima, M., Arai, M., Kagawa, K., Fukutake, K., Kamisue, S., Nakai, H., Morichika, S., Tanaka, I., Inoue, M., Gale, K., Tuddenham, E.G. & Yoshioka, A. (1997) Factor VIII Ise (R2159C) in a patient with mild hemophilia A, an abnormal factor VIII with retention of function but modification of C2 epitopes. *Thrombosis Haemostasis*, **77**, 862–867.

Tagliavacca, L., Moon, N., Dunham, W.R. & Kaufman, R.J. (1997) Identification and functional requirement of Cu(I) and its ligands within coagulation factor VIII. *The Journal of Biological Chemistry*, **272**, 27428–27434.

Takeshima, K., Smith, C., Tait, J. & Fujikawa, K. (2003) The preparation and phospholipid binding property of the C2 domain of human factor VIII. *Thrombosis Haemostasis*, **89**, 788–794.

Takeyama, M., Nogami, K., Okuda, M., Sakurai, Y., Matsumoto, T., Tanaka, I., Yoshioka, A. & Fujikawa, K. (2008) Selective factor VIII and V inactivation by iminodiacetate ion exchange resin through metal ion adsorption. *British Journal of Haematology*, **142**, 962–970.

Vehar, G.A., Keyt, B., Eaton, D., Rodriguez, H., O'Brien, D.P., Rotblat, F., Oppermann, H., Keck, R., Wood, W.I., Harkins, R.N., Tuddenham, E.G.D., Lawn, R.M. & Capon, D.J. (1984) Structure of human factor VIII. *Nature*, **312**, 337–342.

Wakabayashi, H., Koszelak, M.E., Mastri, M. & Fay, P.J. (2001) Metal ion-independent association of factor VIII subunits and the roles of calcium and copper ions for cofactor activity and inter-subunit affinity. *Biochemistry*, **40**, 10293–10300.

Wakabayashi, H., Freas, J., Zhou, Q. & Fay, P.J. (2004) Residues 110–126 in the A1 domain of factor VIII contain a Ca^{2+} binding site required for cofactor activity. *The Journal of Biological Chemistry*, **279**, 12677–12284.

Wakabayashi, H., Su, Y.C., Ahmad, S.S., Walsh, P.N. & Fay, P.J. (2005) A Glu113Ala mutation within a factor VIII Ca^{2+}-binding site enhances cofactor interactions in factor Xase. *Biochemistry*, **44**, 10298–10304.

Wood, W.I., Capon, D.J., Simonsen, C.C., Eaton, D.L., Gitschier, J., Keyt, B., Seeburg, P.H., Smith, D.H., Hollingshead, P., Wion, K.L., Delwart, E., Tuddenham, E.D.G., Vehar, G.A. & Lawn, R.M. (1984) Expression of active human factor VIII from recombinant DNA clones. *Nature*, **312**, 330–337.

Blood Coagulation, Fibrinolysis and Cellular Haemostasis

Identification of a protein S-interactive site within the A2 domain of the factor VIII heavy chain

Masahiro Takeyama[1]; Keiji Nogami[1]; Evgueni L. Saenko[2]; Katsumi Nishiya[1]; Kenichi Ogiwara[1]; Midori Shima[1]

[1]Department of Pediatrics, Nara Medical University, Kashihara, Nara, Japan; [2]Department of Biochemistry and Molecular Biology, University of Maryland School of Medicine, Baltimore, Maryland, USA

Summary

We have recently demonstrated that protein S impairs the intrinsic tenase complex, independent of activated protein C, in competitive interactions between the A2 and A3 domains of factor VIIIa and factor IXa. In the present study, we have identified a protein S-interactive site in the A2 domain of factor VIIIa. Anti-A2 monoclonal antibody recognising a factor IXa-functional region (residues 484–509) on A2, and synthetic peptide inhibited the A2 binding to protein S by ~60% and ~70%, respectively, in solid-phase binding assays. The 484–509 peptide directly bound to protein S dose-dependently. Covalent cross-linking was observed between the 484–509 peptide and protein S following reaction with EDC (1-ethyl-3-(3-dimethylaminopropyl)-carbodiimide). The cross-linked adduct was consistent with 1:1 stoichiometry of reactants. Cross-linking formation was blocked by addition of the 484–497 peptide, but not by the 498–509 peptide. Furthermore, N-terminal sequence analysis of the 484–509 peptide-protein S adduct showed that three sequential residues (S488, R489, and R490) in A2 were not identified, suggesting that these residues participate in cross-link formation. Mutant A2 molecules where these residues were converted to alanine were evaluated for the binding of protein S. The S488A, R489A, and R490A mutants demonstrated ~four-fold lower affinity than wild-type A2. These results indicate that the 484–509 region in the A2 domain of factor VIIIa, in particular sequential residues at positions 488–490, contributes to a unique protein S-interactive site.

Introduction

Factor VIII functions as a cofactor in the tenase complex responsible for anionic phospholipid surface-dependent conversion of factor X to Xa by factor IXa (1). Factor VIII is synthesised as a multi-domain, single chain molecule (A1-A2-B-A3-C1-C2) consisting of 2,332 amino acid residues with a molecular mass of ~300 kDa (2, 3). It is processed into a series of metal ion-dependent heterodimers by cleavage at the B-A3 junction, generating a heavy chain consisting of the A1 and A2 domains, plus heterogeneous fragments of a partially proteolysed B domain, linked to a light chain consisting of the A3, C1, and C2 domains (2–4). Factor VIII circulates as a complex with von Willebrand factor (VWF), which stabilises the cofactor activity of factor VIII (5).

Critical sites for VWF interaction in factor VIII have been localised to the N-terminal acidic region of the A3 domain (6) and the C-terminal region of the C2 domain (7).

The procofactor of factor VIII is activated by cleavage at Arg372, Arg740, and Arg1689 by either thrombin or factor Xa, converting the dimer into the factor VIIIa trimer composed of the A1, A2, and A3C1C2 subunits (8). Proteolysis at Arg372 and Arg1689 is essential for generating factor VIIIa cofactor activity (9). Cleavage at the former site exposes a factor IXa-functional site within the A2 domain that is cryptic in the unactivated molecule (10). Cleavage at the latter site liberates the cofactor from its carrier protein, VWF (11), contributing to the overall specific activity of the cofactor (12). Conversely, factor VIIIa cofactor activity is down-regulated in the presence of serine proteases such

Correspondence to:
Keiji Nogami, MD, PhD
Department of Pediatrics, Nara Medical University
840 Shijo-cho, Kashihara, Nara 634-8522, Japan
Tel.: +81 744 29 8881; Fax: +81 744 24 9222
E-mail: roc-noga@naramed-u.ac.jp

as activated protein C (APC) (8), factor Xa (8), factor IXa (13), and plasmin (14) by proteolytic inactivation following cleavage at Arg336 within A1 subunit.

Protein S, a vitamin K-dependent anticoagulant protein, functions as a cofactor of APC (15), which catalyses the proteolytic inactivation of both factor VIIIa and factor Va on phospholipid membranes (16). The physiological importance of protein S is evident by the clinical observation that its deficiency is associated with a high risk of thrombosis (17, 18). Protein S has also been reported to exhibit anticoagulant activity in the absence of APC. This APC-independent anticoagulation is likely supported by following mechanisms: the inhibition of prothrombin activation via binding of protein S to factor Va (19) and factor Xa (20), and the inhibition of extrinsic tenase activity *via* binding to tissue factor pathway inhibitor (TFPI) of protein S as a cofactor (21, 22). Furthermore, Koppelman et al. (23) reported that protein S also exerted an APC-independent anticoagulant action by inhibiting the intrinsic activation of factor X. On this mechanism, we have recently demonstrated that protein S directly impaired the intrinsic tenase complex by competition with factor IXa for direct binding to both the A2 and A3 domains of factor VIII(a) with similar high affinities (K_d: ~10 nM) (24). In the present study, we have identified a protein S-interactive site within the A2 domain of factor VIIIa using a combination of approaches employing synthetic peptides, antibodies, and recombinant A2 mutants in functional and binding assays. Our results indicate that the 484–509 region in the A2 domain, in particular sequential residues at position 488–490, contributes to a unique protein S-interactive site within the factor VIII heavy chain that promotes protein S docking to the tenase complex.

Materials and methods

Reagents

Recombinant human coagulation factor VIII (Kogenate FS®) donated from Bayer Corporation Japan (Osaka, Japan) was used. The A2 subunit was isolated from factor VIII as previously reported (10). SDS-PAGE of the purified protein followed by staining with GelCode Blue Stain Reagent (Pierce, Rockford, IL, USA) showed >95% purity. Protein concentrations were determined using the Bradford method (25). An anti-A2 mAb, mAb413, which is specific for residues 484–509 in the A2 domain, was obtained as previously described (26). Alternative anti-A2 mAb, mAbJR8, was obtained from JR Scientific Inc. (Woodland, CA, USA). IgG F(ab')$_2$ fragments were prepared using immobilised pepsin-Sepharose (Pierce). Human protein S (Hematologic Technologies, Burlington, VT, USA), 1-ethyl-3-(3-dimethylaminopropyl)-carbodiimide (EDC) (Sigma, St Louis, MO, USA), and horseradish peroxidase-labeled streptavidin (Chemicon, Victoria, Australia) were purchased from the indicated vendors. Synthetic peptides corresponding to factor VIII A2 residues 484–509, and overlapping synthetic peptides with sequences of 12 to 14 residues encompassing this region were prepared by BioSynthesis (Lewisville, TX, USA). Biotinylated 484–509 peptide was also prepared by BioSynthesis. Briefly, the biotin was added to the peptide while all of the side-chains of amino acids with reactive groups were blocked by protecting groups. The N-terminus protecting group (FMOC) was removed and biotin was attached to the N-terminus. The coupling efficiency was checked by Ninhidrin test. Attachment of one biotin to one peptide was confirmed by MS analysis (data not shown).

Recombinant factor VIII A2 molecules

Recombinant wild-type A2 domain (wt-A2) and a set of mutants were constructed and expressed using the Bac-to-Bac baculovirus systems (27). The mutated residues were Tyr487, Ser488, Arg489, and Arg490. Each selected residue was replaced by alanine. The A2 expression cassette was assembled on the basis of an MHGX vector and subcloned into a pFastBac1 vector. The chimeric gene encoded a polypeptide, six His-tag and factor Xa-cleavage site at the N-terminus. The protein was expressed in Sf9 cells and purified by affinity chromatography using anti-A2 mAb. The eluate was mixed with factor Xa and treated with Xarrest agarose (Novagen, Madison, WI, USA). The resultant A2 was >90% pure as judged by SDS-PAGE and western blotting.

Kinetic measurements using real-time biomolecular interaction analysis

The kinetics of protein S interaction with factor VIII A2 subunit were determined by surface plasmon resonance (SPR)-based assays using a BIAcore X instrument (BIAcore AB, Uppsala, Sweden) (24). Protein S was covalently coated to the CM5 chip at a coupling density of ~4 ng/mm². Association of the ligand was monitored in the running buffer (10mM HEPES pH 7.4, 0.1 M NaCl, 1 mM CaCl$_2$, 0.005% polysorbate 20) for 2 min at a flow rate 20 μl/min. The dissociation of bound ligand was recorded over a two minutes period by replacing the ligand-containing buffer with buffer alone. The level of nonspecific binding corresponding to the ligand binding to the uncoated chip was subtracted from the signal. Reactions were performed at 37°C. Rate constants for association (k_{as}) and dissociation (k_{diss}) were determined by nonlinear regression analysis using evaluation software provided by BIAcore AB. Dissociation constants (K_d) were calculated as k_{diss}/k_{as}.

ELISA for binding of the A2 or 484–509 peptide to protein S

Microtiter wells were coated with protein S (200 nM) in 20 mM Tris and 0.15 M NaCl, pH 7.4, overnight at 4°C. The wells were washed with PBS containing 0.01% Tween 20 and were blocked with PBS containing 5% human serum albumin (HSA) for two hr at 37°C. Various amounts of the A2 subunit or biotinylated 484–509 peptide were then added in Hepes-buffered saline (HBS)-buffer (20 mM HEPES, pH 7.2, 0.1 M NaCl, 0.01% Tween 20) containing 1 mM CaCl$_2$, and 1% HSA for 2 hours at 37°C. Bound A2 or peptide was quantified by the addition of biotinylated anti-A2 mAb and/or horseradish peroxidase-labeled streptavidin and *O*-phenylenediamine dihydrochloride substrate. Reactions were quenched by the addition of 2 M H$_2$SO$_4$, and absorbances were measured at 492 nm using microplate reader. The amount of non-specific binding of anti-A2 mAb or streptavidin in the absence of A2 or biotinylated peptide, respectively, was <3% of the total signal. Specific binding was recorded after subtracting the nonspecific binding.

Cross-linking with EDC

Cross-linking reactions were run in HBS buffer containing 1 mM CaCl2 at 22°C for the indicated times. Reactions were terminated by addition of SDS electrophoresis sample buffer and boiling for three min.

Electrophoresis and Western blotting

SDS-PAGE was performed using eight percent gels at 150 V for one hour (28). For Western blotting, the proteins were transferred to a polyvinylidene difluoride (PVDF) membrane at 50 V for two hours in buffer containing 10 mM 3-(cyclo-hexylamino)-1-propanesulfonic acid (CAPS), pH 11 and 10% (v/v) methanol. Proteins were probed using horseradish peroxidase-labeled streptavidin. The signals were detected using an enhanced chemiluminescence system (PerkinElmer Life Science, Boston, MA, USA). Densitometry scans were quantitated using Image J 1.34 (National Institute of Health, USA).

Amino acid sequencing of cross-linked 484–509 peptide and protein S

Protein S (150 nM) was incubated with the unlabeled 484–509 peptide (200 μM) for 30 min at 22°C. EDC (2 mM) was added to the reactant and incubation was further continued for 1 hr at 22°C. After the addition of SDS sample buffer and boiling, the mixture was subjected to electrophoresis on 8% gels. Proteins were transferred to PVDF membrane at 50 V for 2 hr in buffer containing 10 mM CAPS, pH 11 and 10% (v/v) methanol, and 0.5 M dithiothretiol. The blots were stained with 0.2% Coomassie brilliant blue in 40% methanol and 10% acetic acid for 10 minutes. Individual bands were excised and sequenced using an Applied Biosystems Model 491 Sequencer (Foster City, CA, USA).

Data analyses

All experiments were performed at least three separate times, and the average values and standard deviations were shown. Non-linear least squares regression analyses were performed by Kaleidagraph (Synergy Reading, PA). Analyses of the interactions between the A2 (or A2 peptide) and protein S in ELISA were performed by a single-site binding model using Equation 1,

$$\text{Absorbance} = \frac{A_{max} \cdot [S]}{K_d + [S]}$$

where [S] is the concentration of A2 subunit or peptide in the solid phase binding assay; K_d is the dissociation constant; and A_{max} represents maximum absorbance signal when the site is saturated by the A2 or peptide.

Data from studies assessing the A2 peptide-dependent inhibition of protein S interaction with A2 subunit were fitted by nonlinear least squares regression by using Equation 2,

$$\% \text{ binding} = \frac{B_{max} \cdot [A2]}{K_d \cdot \left[1 + \dfrac{[L]}{K_i}\right] + [A2]} + C$$

where L represents the concentration of A2 peptide or protein S; B_{max} represents maximum binding; K_d is the dissociation constant for the interaction between the A2 and protein S; K_i is the apparent inhibition constant for L; and C is a constant for binding of the A2 and protein S that was unaffected by L.

Results

Inhibition of the A2 subunit and protein S interaction by anti-A2 mAb413

We have recently demonstrated that protein S directly impairs the tenase complex by competition with factor IXa for direct binding to both the A2 and A3 domains of factor VIII(a) in APC-independent anticoagulant mechanisms (24). Since the A2 domain is commonly recognised to be more prominent than A3 in the regulation of factor VIII(a) function, we attempted, in the present study, to localise the protein S-interactive site(s) on the A2 domain involved in anticoagulant reactions. A factor IXa-functional site on the A2 domain is located within the 484–509 region, and an anti-A2 mAb413 recognising this epitope inhibits the A2-factor IXa association (29). Therefore, we first examined the effect of this antibody on the A2 binding of protein S in SPR-based assays. We have recently utilised this approach to confirm that the A2 domain directly binds to immobilised protein S with high affinity (24). Isolated A2 subunit preparations (200 nM) were preincubated with various concentrations of mAb413 F(ab')2 and added to protein S immobilised on the sensor chip. In control experiments, this antibody did not directly bind to protein S (data not shown). The mAb413 inhibited the A2 binding to protein S in a dose-dependent manner (Fig. 1A, inset). Calculation of the optimum response at 120 seconds after the addition of reactant mixture showed that the inhibitory effect was ~60% at the maximum antibody concentrations (5 μM, Fig. 1A). In contrast, an anti-A2 mAbJR8, which does not overlap with the epitope of mAb413, did not significantly inhibit this interaction. This finding supported that a protein S-interactive site on the A2 domain might overlap or juxtapose the factor IXa-functional site at residues 484–509.

Effect of the 484–509 peptide on the A2 subunit-protein S interaction

We further evaluated the A2-protein S interaction using an alternative binding assay. Various concentrations of the A2 subunit were added to protein S (200 nM) immobilised onto microtiter wells, and bound A2 was detected using biotinylated anti-A2 (JR8) mAb IgG, which did not affect A2-protein S binding. Control experiments to detect immobilised protein S using an anti-protein S mAb showed that immobilised protein S was not affected by the ionic strength of the wash buffer, duration of the wash, and incubation steps subsequent to protein S binding (data not shown). Reactions of the A2 subunit with protein S yielded saturable binding curves (Fig. 1B), and the data were well-fitted in a single-site binding model. This method is not based on a true equilibrium binding assay, however, and the K_d values obtained represent an apparent K_d for the interactions. Nevertheless, the K_d value (25.5 ± 4.2 nM) obtained for this interaction was similar to that obtained from the SPR-based assay (~12 nM [24]). To confirm the specificity of this binding, various concentrations of
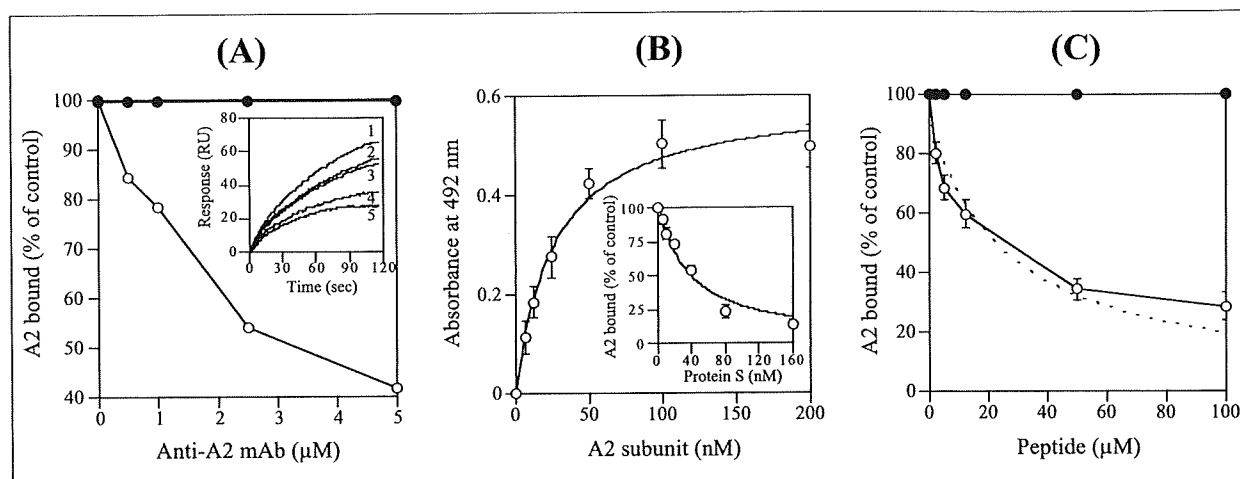
(A) **(B)** **(C)**

Figure 1: Effect of anti-A2 mAb or A2 peptide on the A2 sub-unit binding to protein S. A) Effect of anti-A2 mAb in SPR-based assay: The A2 subunit (200 nM) was preincubated with various concentrations of anti-A2 mAb413 (O) or mAbJR8 (●) for 1 h, followed by the addition of reactant mixtures to protein S immobilised on the sensor chip in an SPR-based assay. Inset shows the association curves of A2 subunit incubated with mAb413 (Lines 1–5; 0, 0.5, 1.0, 2.5 and 5 μM, respectively). Data represent relative responses in the presence of anti-A2 mAb, based on the association curve obtained by this assay. A maximal response value in the absence of anti-A2 mAb was used to represent the 100% level. B) ELISA for A2 binding to protein S: Various concentrations of isolated A2 were reacted with protein S (200 nM) immobilised onto micro-titer wells. Bound A2 was detected using biotinylated anti-A2 mAbJR8. Data were fitted using the Equation 1 according to a

single-site binding model. Inset) The mixtures of A2 (40 nM) and various concentrations of protein S were incubated with immobilised protein S. Absorbance value corresponding to A2 binding to protein S in the absence of competitor was defined as 100%. The plotted data were fitted by non-linear least squares regression according to Equation 2. C) Effect of the 484–509 peptide in ELISA: The A2 subunit (40 nM) was mixed with various concentrations of the 484–509 peptide (O) or scrambled peptide (●) and the mixtures were then incubated with immobilised protein S (200 nM). Bound A2 was detected using biotinylated mAbJR8. Absorbance value corresponding to A2 binding to protein S in the absence of competitor was defined as 100%. The plotted data were fitted (dashed line) by non-linear least squares regression according to Equation 2.

protein S were preincubated with the isolated A2 (40 nM) in the fluid phase prior to addition to the immobilised protein S. Protein S significantly blocked the A2-protein S interaction (Fig. 1B, inset). The K_i value (22.4 ± 3.9 nM) was similar to the K_d value obtained from direct binding, confirming the specificity of this assay. Furthermore, to assess the specificity of the 484–509 region in A2 for the protein S interaction, we examined the inhibitory effect of the 484–509 peptide on this fluid-phase interaction (Fig. 1C). This peptide inhibited the A2-protein S interaction in a dose-dependent manner. Inhibition was ~70% at the maximum concentration employed (100 μM), and the K_i value obtained was 18.6 ± 5.5 μM. In contrast, control experiments using peptides with scrambled sequences (RPY-DIPVFEHRLSLKLKRPLGFIGKP) based on 484–509 showed little inhibition of binding. These findings confirmed that residues 484–509 in the A2 domain participated in protein S interaction.

Direct binding of the 484–509 peptide to protein S

To obtain direct evidence that residues 484–509 in the A2 domain contains a protein S-interactive site, direct binding between this peptide and protein S was quantified using two approaches: SPR-based assay and ELISA. Peptide-protein S interaction was low affinity, and it was difficult to determine reliable K_d values from the kinetic parameters obtained by SPR-based assays. In

these circumstances, therefore, maximum responses (RU) were determined by the addition of various concentrations of peptide. These RU values were shown to be dose-dependent, and the data were well-fitted using a single-site binding model (Fig. 2A). The K_d value obtained was 29.8 ± 2.6 μM, similar to the K_i value (~20 μM) for peptide on the A2-protein S interaction as described above. In contrast, a control peptide with scrambled sequences demonstrated little binding. In the ELISA, 484–509 peptide labeled with biotin was utilised in place of native peptide for detection of bound peptide. The labeled peptide also bound to immobilised protein S directly in a dose-dependent manner (Fig. 2B), with an apparent K_d value of 107 ± 11 μM. These results strongly suggested that residues 484–509 in the A2 domain contributed to protein S binding. However, the unlabelled peptide possessed a ~four-fold higher affinity for protein S in SPR-based assays compared to that of the biotinylated reagent in ELISA. Although different assays were used, the findings might indicate some inhibition of the intermolecular interaction by the biotin label.

Restriction of a protein S-interactive site within the 484–509 region

To further localise the protein S-interactive site within the 484–509 region, a competitive binding ELISA was developed using overlapping synthetic peptides encompassing amino acid
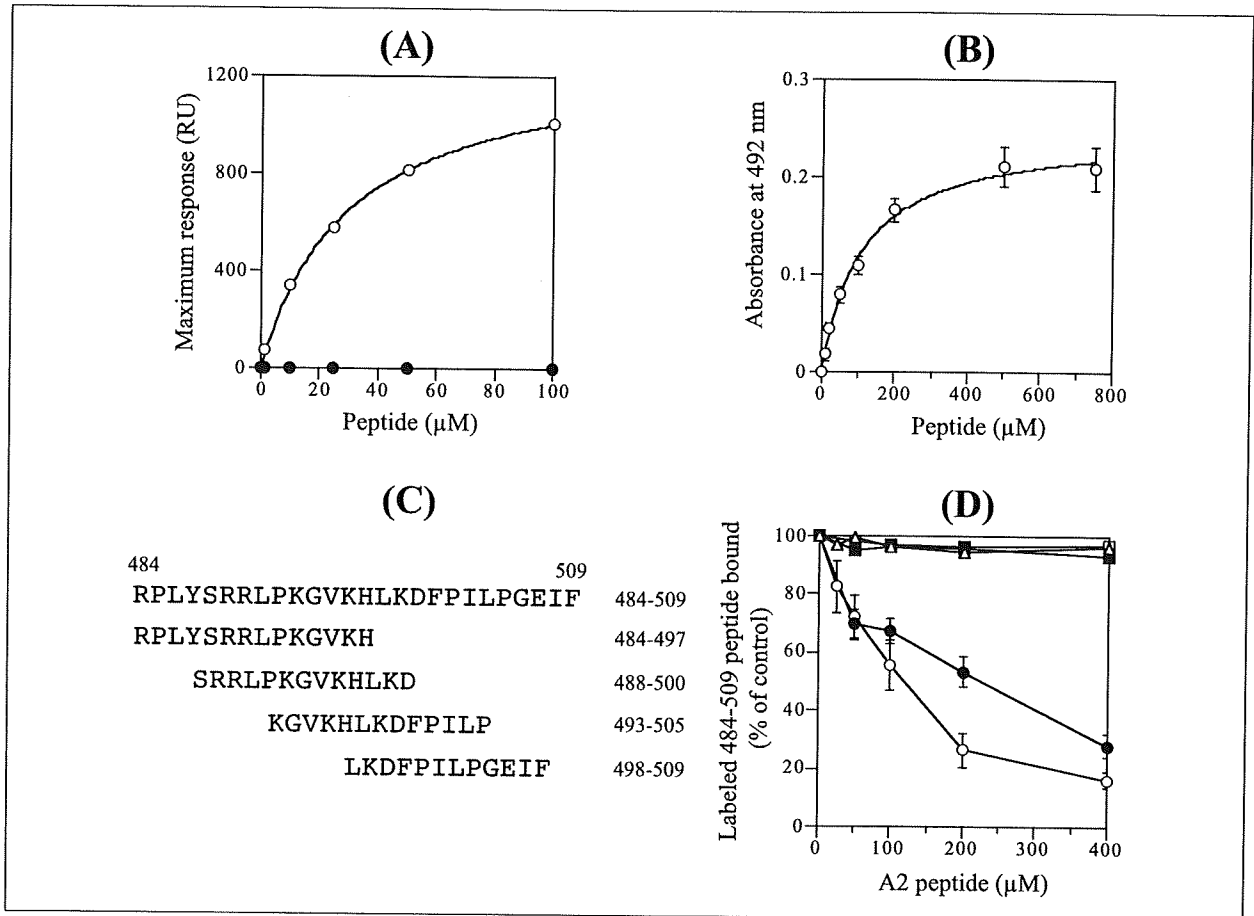
(A)

(B)

(C)

```
484                                    509
RPLYSRRLPKGVKHLKDFPILPGEIF    484-509

RPLYSRRLPKGVKH               484-497

    SRRLPKGVKHLKD            488-500

      KGVKHLKDFPILP          493-505

          LKDFPILPGEIF       498-509
```

(D)

Figure 2: Direct binding of the 484–509 peptide to protein S.
A) SPR-based-assay: Various amounts of the 484–509 peptide (O) or scrambled peptide (●) were added to immobilised protein S on a sensor chip, followed by a change of running buffer for 2 min. Maximum values for association of the 484–509 peptide were plotted as a function of A2 peptide concentration, and the plotted data were fitted using the Equation I according to a single-site binding model. B) ELISA: Various concentrations of biotinylated 484–509 peptide were incubated with immobilised protein S (200 nM). Bound peptide was detected using peroxidase-labeled streptavidin. The plotted data were fitted using the Equation I according to a single-site binding model. C) Schematic repre-

sentation of the synthetic A2 peptides: The sequences of the A2 peptide in the residues 484–509 are represented by their I-letter abbreviations. D) Inhibitory effects of A2 peptides on the 484–509 peptide-protein S binding in ELISA: The mixtures of biotinylated 484–509 peptide (200 μM) and various concentrations of unlabeled A2 peptides were incubated with immobilised protein S (200 nM). Bound biotinylated peptide was detected using peroxidase-labeled streptavidin. Absorbance value corresponding to biotinylated 484–509 peptide binding to protein S in the absence of competitor was defined as 100%. The symbols used are as follows: 484–509 peptide (O), 484–497 peptide (●), 488–500 peptide (□), 493–505 peptide (■), and 498–509 peptide (Δ).

sequences within these residues (Fig. 2C). Various amounts of overlapping peptides were mixed with the biotinylated 484–509 peptide (200 μM) in the fluid phase, prior to addition to the immobilised protein S. Control experiments showed that the unlabeled 484–509 peptide significantly blocked (by ~90%) the binding of labeled peptide to protein S (Fig. 2D), confirming the specificity of this assay. The 484–497 peptide, the former region of 484–509 sequences, also blocked this binding in a dose-dependent manner by ~80% at maximum concentrations employed. The IC_{50}(half maximal inhibitory concentration) value was ~220 μM, although this level of inhibition was somewhat weaker than that of the 484–509 peptide (IC_{50}; ~110 μM). How-

ever, the 498–509 peptide, corresponding to the latter region, did not significantly inhibit this binding. In addition, the 488–500 and 493–505 peptide did not affect binding even at the maximum concentrations employed. The results suggested that the 484–497 sequence in particular within the A2 484–509 region could represent a protein S-interactive site.

Zero-length cross-linking of the 484–509 peptide and protein S

Nogami et al. (30) reported that the 337–372 peptide in the C-terminus of A1 formed a covalent, cross-linked product with factor Xa. To monitor the direct interaction between the 484–509 pep-
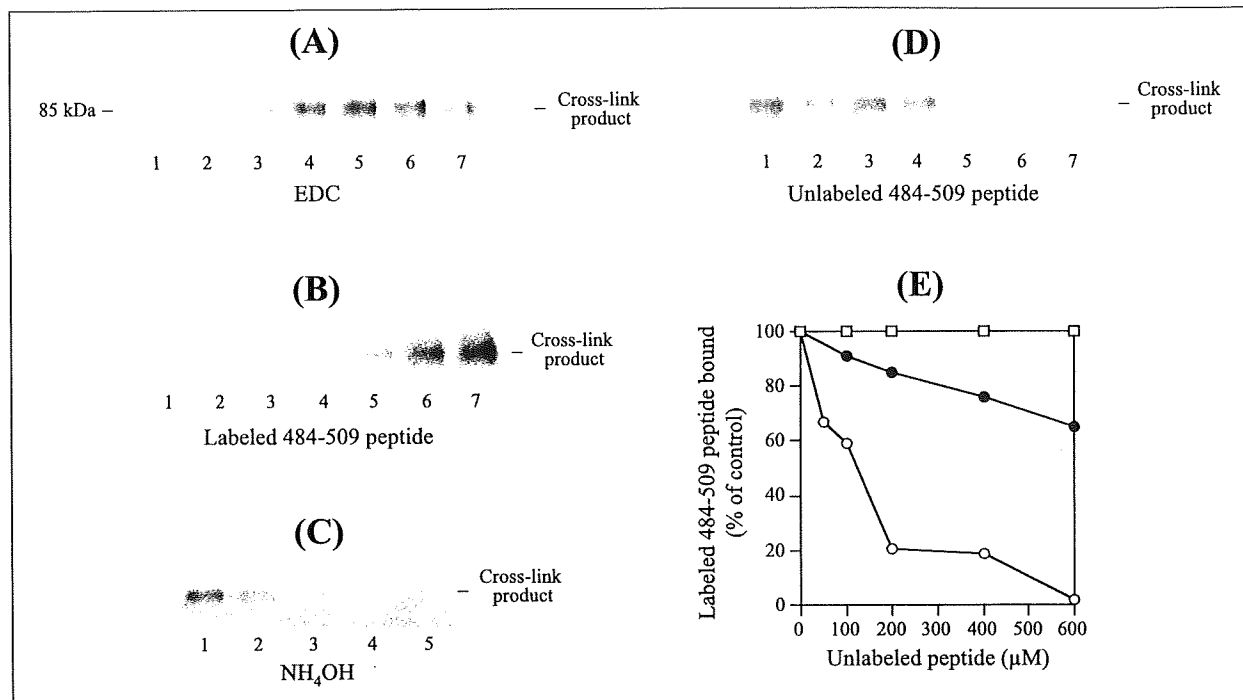
Figure 3: EDC cross-linking of the 484–509 peptide and protein S. A) Protein S (150 nM) was incubated with biotinylated 484–509 peptide (200 μM) in the presence of various amounts of EDC (lanes 1–7; 0, 0.2, 0.5, 1, 2, 5, and 10 mM, respectively) for 2 hrs, followed by immunoblotting using streptavidin. B) Cross-linked products formed with protein S (150 nM) and various concentrations of the 484–509 peptide (lanes 1–7; 0, 12, 25, 50, 100, 200, and 400 μM, respectively) with EDC (2 mM). C) Cross-linked products formed with protein S (150 nM) and biotinylated 484–509 peptide with EDC (2 mM) in the presence of NH4OH (lanes 1–5; 0, 50, 100, 200, and 400 μM, respectively). D) Protein S (150 nM) and biotinylated 484–509 peptide (200 μM) reacted with EDC (2 mM) in the presence of unlabeled 484–509 peptide (lanes 1–7; 0, 25, 50, 100, 200, 400, and 600 μM, respectively) and were immunoblotted. E) Densitometry was used to quantify inhibition of the reaction run in panel D with unlabeled 484–509 peptide (O), 484–497 peptide (●), and 498–507 peptide (□).

tide and protein S in a fluid phase, we performed experiments using the zero-length cross-linking reagent EDC. This reagent initially reacts with the carboxyl group on a carboxylic acid residue to form an unstable O-acylisourea adduct which can react with a nearby ε-amino group of Lys or hydroxyl group of nucleophile such as Ser or Thr to form an isoamide or ester linkage, respectively (31). Protein S (150 nM) in the presence of biotinylated 484–509 peptide (200 μM) was incubated with various concentrations of EDC at 22°C for two hours. Following this cross-linking protocol, samples were subjected to SDS-PAGE, transferred to PVDF, and immunoblotted with streptavidin. Results (Fig. 3A) showed a dose-dependent formation of an ~85 kD product, indicating a covalent cross-link between the 484–509 peptide and protein S. The mass of the adduct (~85 kD) was consistent with a one-to-one stoichiometry of the peptide (~4 kD) and protein S (~80 kD). At higher amounts of EDC (>5 mM), however, we observed loss of band density. The reason for this is unknown but may result from formation of covalent aggregates that fails to resolve in the gels and/or transfer. In addition, various concentrations of biotinylated 484–509 peptide were incubated with protein S (150 nM) with EDC (2 mM) under same conditions. Cross-linked adducts were again observed in a dose-

dependent manner (Fig. 3B). Control experiments showed that no cross-linked product was formed between biotinylated 484–509 peptide and bovine serum albumin (data not shown).

The nature of the chemical linkage of the peptide-protein S product was investigated by treating samples with NH4OH subsequent to the cross-linking procedure. Cross-linking diminished in intensity by the alkaline treatment, compared to the untreated samples, as determined by Western blot analysis (Fig. 3C). Isoamide linkages formed by cross-linkage with ε-amino group of Lys are base-resistant, and these findings indicated the likely presence of ester linkages between the carboxyl groups of acidic residues and hydroxyl group of nucleophile residues. The number of possible ester linkages and the presence isoamide bonds in the cross-linked adduct remain to be determined.

The specificity of the interaction between the 484–509 peptide and protein S as monitored by cross-linking was examined using unlabeled peptide to block formation of the biotinylated peptide-protein S compound. Various concentrations of unlabeled peptides were combined with fixed concentrations of protein S (150 nM) and biotinylated 484–509 peptide (200 μM), and the mixtures were reacted with EDC (2 mM) as above. Figure 3D illustrates the loss of biotinylated product following titration
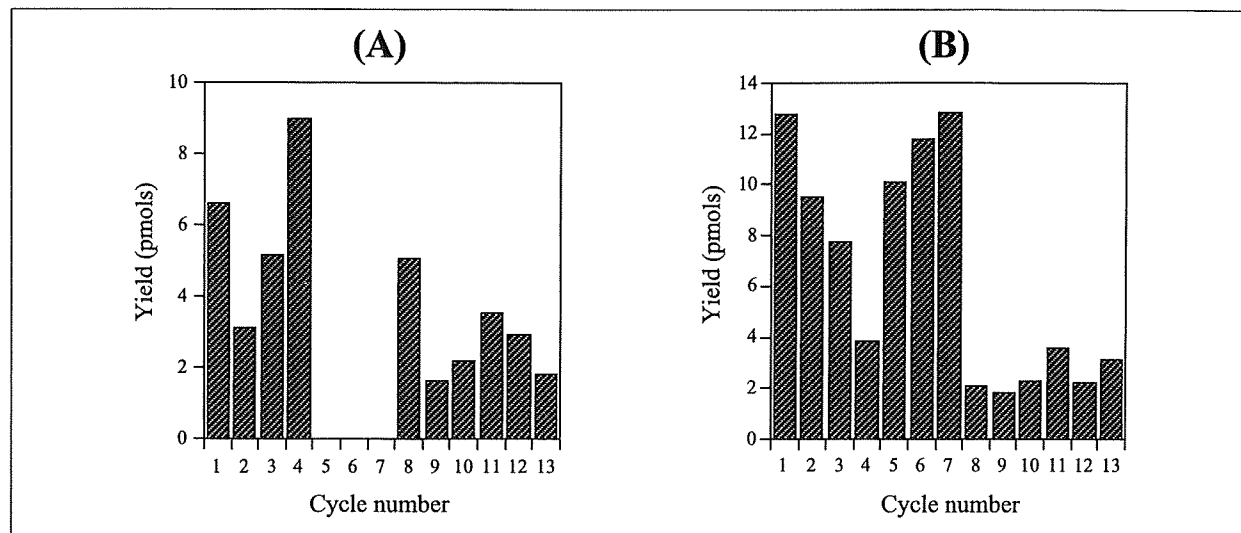
(A) **(B)**

Figure 4: Sequence analysis of the cross-linked product between 484–509 peptide and protein S. Results are presented as subtraction chromatograms wherein the yield (in picomoles [pmol]) for a given residue (except the initial residue) was reduced from the value for that residue in the previous cycle. Experiments were performed twice, and the bar graph shows the average value of residue yield for each cycle. A) Residue yields attributed to the 484–509 peptide sequence; B) Residue yields attributed to the protein S sequence. For panel A, the peptide sequence for 13 cycles, using the single letter code, corresponds to RPLY(S)(R)(R)LPKGVK. For panel B, the protein S sequence is ANSLLEETKQGNL. Ser (S), Arg (R), and Arg (R) were not identified at cycles 5–7, respectively, of the 484–509 peptide sequence.

with the unlabelled 484–509 peptide, and this response was quantitated by densitometry (Fig. 3E). Unlabelled 484–509 peptide (600 μM) completely inhibited formation of the EDC cross-linking product between the biotinylated 484–509 peptide and protein S. The IC_{50} value for this inhibition was ~120 μM. The 484–497 peptide modestly inhibited the formation of this product (by ~40%), whilst the 498–509 peptide showed little inhibition. These data were keeping with the specificity of the interaction between the A2 484–509 region and protein S and the restriction of the interactive site within residues 484–497.

N-terminal sequence analysis of peptide-protein S cross-linked product

In an attempt to determine the specific residues in the 484–509 peptide that form cross-links with protein S, N-terminal peptide sequence analysis of the peptide-protein S adduct was performed, as described by O'Brien et al (32). Cross-linked materials were obtained following reaction of unlabelled peptide (200 μM), protein S (150 nM), and EDC (2 mM). After transferring to PVDF, the bands corresponding to cross-linked product were excised and subjected to sequence analysis. Since the peptide-protein S compound contains two N-termini, each cycle of sequencing releases a residue from each chain. The residues identified by this analysis matched the predicted residues for the N-termini of the 484–509 peptide and protein S. Figure 4 shows the sequence data (in picomole residue recovered) with results obtained for peptide in Figure 4A and protein S in Figure 4B. Two analyses using different preparations of material were performed and the average data are shown. Residues were not resolved beyond 13 cycles, however, possibly due to similar yields of the two resi-

dues, limited amount of material available for this analysis and/or high background levels resulting from simultaneous analysis of two N-termini. The similar yields of residues from each of the two N-termini supported the view that the peptide and protein S were associated in a 1:1 stoichiometry. Interestingly, Ser488, Arg489, and Arg490 (expected in sequencing cycles no.5–7, respectively) were not detected in the peptide during the sequencing of the two cross-linked preparations. Sequence analysis of the native peptide (data not shown) had confirmed that Ser488, Arg489, and Arg490 were obtained in cycles number five to seven with yields consistent with other identified residues. In contrast, yields of all expected residues for the 13 cycles of protein S were detectable. Residues involved in a covalent linkage resulting from cross-linking were not detected, this resulting in a gap in the sequences of that chain (32). Therefore, we tentatively concluded that Ser488, Arg489, and Arg490 in the peptide could form the cross-links with a yet unidentified carboxylic acid residue in protein S, although interpretation of this data is limited.

Protein S interaction with the A2 mutants in a SPR-based assay

To further confirm that the three sequential residues, Ser488, Arg489, and Arg490, in the A2 domain were responsible for interaction with protein S, a series of recombinant mutant A2 molecules were prepared using a baculovirus expression system (27). These residues were converted to alanine, generating a panel of three single-point A2 mutants. The secretion levels and conformational stabilities of the A2 mutants, and specific activities of factor VIIIa obtained from reconstituted mutated A2 and A1/A3C1C2 dimers have been previously described (27). Inter-
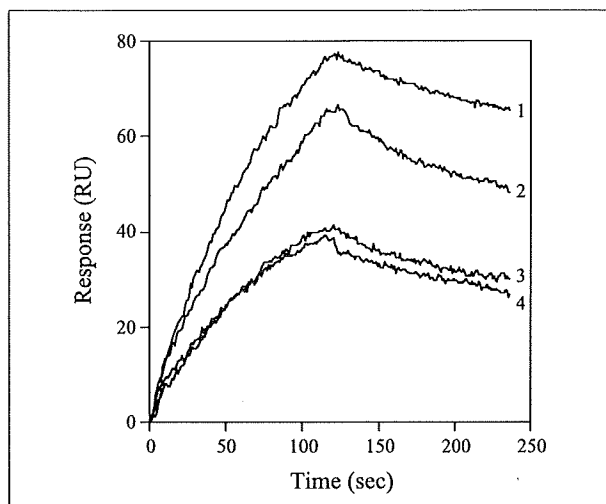
Figure 5: Binding of recombinant A2 mutants to protein S in an SPR-based assay. Recombinant wt-A2 or its mutants (200 nM) were incubated with protein S immobilised on a sensor chip, followed by a change of running buffer for two minutes. Curves 1–4 show the representative association/dissociation curves of wt-A2, and its mutants, S488A, R489A, and R490A, respectively.

Table I: Binding parameters determined for the interaction of A2 mutants and protein S in an SPR-based assay. Reactions were performed as described under "Materials and methods". Parameter values were calculated by nonlinear regression analysis using the evaluation software provided by Biacore AB. #: Values were calculated as k_{diss} / k_{as}. *: not determined.

A2 mutant	k_{as}	k_{diss}	K_d #
	$\times 10^4\ M^{-1}s^{-1}$	$\times 10^{-3}\ s^{-1}$	nM
Wild type	12.3 ± 1.7	1.2 ± 0.6	9.6
Y487A	11.9 ± 3.1	1.5 ± 0.6	12.5
S488A	8.4 ± 1.4	2.6 ± 0.4	31.9
R489A	6.0 ± 1.2	2.3 ± 0.8	40.4
R490A	6.7 ± 1.3	2.5 ± 0.4	40.4

actions between the A2 mutants and protein S were evaluated using SPR-based assays (Fig. 5 and Table 1). The data were comparatively well-fitted by non-linear regression using a one-to-one binding model with mass transfer. The binding affinity of wild-type A2 (wt-A2) for protein S was equivalent to that obtained for plasma-derived isolated A2 (9.6 nM [24]), indicating that the arrangement of the protein S-interactive site was similar in both preparations. Binding of S488A, R489A, and R490A mutants to protein S (K_d: 31.9, 40.4, and 40.4 nM, respectively) demonstrated ~four-fold lower affinities than that of wt-A2, confirming that the A2 residues 488–490 play a major role in protein S binding. The data were consistent with the results obtained above using EDC cross-linking. A control experiment showed

that the Y487A mutant, the neighbouring Tyr487 residue converted to alanine, bound to protein S with an affinity similar to that of wt-A2. Furthermore, we tried to prepare recombinant mutant A2 molecule, generating a triple mutation of Ser488, Arg489, and Arg490 to alanine. However, the triple mutant failed to be expressed. Collectively, these results suggested that the sequential residues of Ser488, Arg489, and Arg490 were significantly involved in A2 binding to protein S.

Discussion

Residues 484–509 in the factor VIII A2 domain comprise a highly basic spacer region exposed on the molecular surface and are known to contain a functionally critical region participating in several protein-protein (or protein-protease) interactions. In the present context, this sequence is implicated in the association with factor IXa and the regulation of factor Xase activity (26). This region also represents a major epitope for factor VIII inhibitor antibodies developed in multi-transfused haemophilia A patients (26), and hence plays an important role in factor VIII function. Antibodies recognising residues 484-509 block the association between the A2 domain and factor IXa (29). Furthermore, clearance of activated factor VIII (factor VIIIa) from the circulation is promoted by the binding of this region to the hepatic clearance receptor, low-density lipoprotein receptor-related protein (LRP) (27). In addition, we have recently reported that this region in the A2 domain contributes significantly to plasmin (33) and thrombin (34) docking, mediating proteolytic activity. These diverse studies show that residues 484–509 in A2 play a vital role in factor VIII metabolism *in vivo*. Results presented in the current study employing a combination of functional approaches demonstrated that this basic region also constitutes an interactive site for protein S-binding.

Direct binding between the 484–509 peptide and protein S was evident using two independent experimental techniques, utilising ELISA and SPR-based principles, and the specificity of binding was confirmed in competitive inhibition assays using unlabelled peptide. Furthermore, a range of overlapping (or substituted) peptides, zero-length cross-linking methods and site-directed mutagenesis showed that a unique protein S-binding site within 484–509 was restricted, in particular, to residues 488–490. Interestingly, competitive assays showed that the 484–497 peptide containing the sequence SRR partially inhibited binding, whilst the 488–500 peptide with SRR failed to moderate the reaction. These results using overlapping peptides suggested that the association between the 484–509 A2 region and protein S might be governed by sites spanning the 488–490 residues and/or might be dependent on a conformation exhibited only in the full length peptide (484–497 peptide).

Our recent findings indicated that protein S, the A2 domain of factor VIIIa and factor IXa competitively interacted in an APC-independent anticoagulant mechanism (24). In addition, earlier studies had demonstrated that mAb413 with a 484–509 epitope overlapping the factor IXa-functional site, inhibited A2-protein S interaction, and for these reasons we attempted the identification of the protein S-binding site using synthetic peptide corresponding to this sequence. Interestingly, residues Arg489 and Arg490 among the identified three residues were

consistent with the crucial residues in factor IXa-functional site. Recent evidence by Jenkins et al. (35) suggested that two sequential residues play a significant role in factor IXa-interactions, modulating the basic electrostatic potential in facilitating catalysis (kcat) rather than affinity (Km). Alternative factor IXa-interactive sites in the A2 domain have been localised within the residues 556–565 (36) and 708–715 (37) on the extended A2 surface. In our study, however, A2 peptides corresponding to these latter regions had little effect on the A2-protein S interaction (data not shown). Our observations indicated, therefore, that the 484–509 region contains a major protein S-interactive site in A2, although the presence of unidentified binding regions cannot be excluded.

The formation of covalent bonds between the 484–509 peptide and protein S in the presence of the zero-length cross-linking reagent, EDC, is in keeping with our recent suggestion that interactions between A2 and protein S are highly sensitive to ionic strength and primary electrostatic forces (24). Furthermore, cross-linking was base-sensitive, indicating an ester linkage between carboxylic acid and the hydroxyl group of nucleophile amino acids such as Ser or Thr. The 484–509 sequence in A2 includes clustered basic residues and two scattered acidic residues (see Fig. 4). In addition, using sequence analyses, we identified the three sequential residues discussed above (Ser488, Arg489, Arg490) as pivotal in the cross-liked product. Based on these data, we suggest that Ser488 provides the central hydroxyl residue in A2 for EDC cross-linking with carboxylic acid(s) in protein S. However, the presence of a base-resistant, isoamide-type linkage, in addition to the ester-type linkage, cannot be completely excluded. The binding affinity (K_d ~10 nM) for the A2-protein S interaction correlates with the estimate of thermodynamic stability (~11.3 kcal/mol), whereas the free energy of a charged or ion pair of hydrogen bonds ranges from 3 to 6 kcal/mol (38). It seems likely, therefore, that an ionic (salt) bridge contributes a significant part of the binding energy in A2-protein S interactions. Unfortunately, the direct EDC cross-linking of whole A2-protein S failed to detect (data not shown). A steric hindrance caused by protein-protein interaction may interfere with the formation of cross-linking, since the spacer arm of EDC is too short.

LRP-, plasmin- and thrombin-binding site(s) have been localised in the A2 domain using single point A2 mutants (27, 33, 34). This study, three A2 mutants, S488A, R489A, and R490A, reduced the affinity of A2 binding to protein S by ~four-fold compared to wt-A2. In addition, peptide 484–509 488/489/490Ala, in which Ser488, Arg489, and Arg490 were each converted to alanine, minimally inhibited interaction between A2 and protein S. These observations were consistent with the three residues identified by sequence analysis of the cross-linked product. Significant conformational disturbances are unlikely in mutants of this nature (27), and the data strongly suggested, therefore, that residues Ser488, Arg489, and Arg490 were the major functional determinants for the protein S-binding site in A2. All three residues together may have a synergistic effect. However, we could not confirm this in this study, since we failed to prepare the triple mutant.

The factor VIII domain structure based on the homology with ceruloplasmin (39) indicates that these residues are exposed on the A2 surface. It may be significant that comparisons of amino acid sequences among human, porcine, murine, and canine factor VIII molecules (http://europium.csc.mrc.ac.uk) suggest that Arg490 is well-conserved and that Ser488 and Arg489 have less inter-species homology (Ser/Arg, Pro/Gly, Ala/Arg, and Thr/Gly, respectively). It is possible, therefore, that specific interaction mechanisms involving protein S and the factor VIII A2 domain may be species-dependent, and other species may have compensatory changes in sequence for the binding site on protein S.

Factor VIIIa and factor Va are structurally and functionally homologous (40). Protein S interacts with both factor Va and factor VIIIa through APC-independent anticoagulant mechanisms (19, 23). However, the region in factor Va corresponding to the 484–509 region in factor VIIIa possessed a low level of homology. Heeb et al. (41) demonstrated that a protein S-binding site in factor Va was localised within the 493–506 residues in the A2 domain. This region (GLLLICKSRSLDRR) is rich in basic residues and juxtaposes the APC-cleavage site at Arg506. The 549–564 region in factor VIIIa (GPLLICYKESVDQR) involves the APC-cleavage site at Arg562 and possesses a similar sequence to 493–506 in factor Va. The previous report suggested, however, that the 549–564 region in factor VIIIa did not constitute a binding site for protein S (41), and our studies also demonstrated that the peptide corresponding to this sequence in factor VIIIa failed to bind significantly to protein S (data not shown). The 484–509 peptide that did bind to protein S is composed of a different sequence. It seems likely, therefore, that the protein S-binding reaction involving the A2 domain in factor VIIIa is distinct from that in factor Va, although both factors function in APC-independent anticoagulant mechanisms.

Approximately 50% of the protein S in plasma is bound to C4b-binding protein. Sites for the interaction with C4b-binding protein have been reported in the steroid hormone-binding domain of protein S at residues 413–433 (42) and 447–460 (43). The A2-protein S interaction does not appear to be significantly affected by the presence of C4b-binding protein (unpublished

---

What is known about this topic?
− Protein S functions as a cofactor of APC, which catalyses the proteolytic inactivation of factor VIIIa.
− Protein S has also been reported to serve as an APC-independent direct anticoagulant. This mechanism is due to impairment of the tenase complex by competitive interactions between the A2 and A3 domains of factor VIIIa and factor IXa.

What does this paper add?
− We have identified a protein S-interactive site in the A2 domain of factor VIIIa using a combination of approaches employing synthetic peptides, antibodies, and recombinant A2 mutants in functional and binding assays.
− We demonstrate that the 484–509 region in the A2 domain, in particular residues 488–490, contributes to a unique protein S-interactive site within the factor VIII heavy chain.

data). In addition, N-terminal sequence analysis of EDC cross-linked product showed residues 1–13 (ANSLLEETKQGNL) in protein S did not bind to the 484–509 region, supporting that these three regions in protein S are unlikely essential for interaction with the A2 domain. On the other hand, Heeb et al. (44) reported that C-terminal residues 621–635 of protein S comprise a binding site for factor Va heavy chain. A direct interaction between this site and the 493–506 region in factor Va seems unlikely, however, since both sites have a substantial net positive charge. Overall, the evidence indicates that protein S and factor Va probably have more than one site of molecular interaction. Since the 484–509 region in factor VIIIa A2 domain also has a net positive charge, this region would interact with the acidic region involving carboxylic acid(s), except for the 621–635 region.

In the present study we have identified a novel protein S-interactive site within the A2 domain of factor VIIIa. Protein S moderates the interaction between factor VIIIa and factor IXa in the down-regulation of factor Xa in the tenase complex, and the present findings provide further information on this direct anti-coagulant mode of action. The physiological role of the 484–509 region of factor VIIIa in the function of protein S as a cofactor of APC (APC-dependent mechanism) remains to be determined, however. In addition, protein S also inhibits interactions between the factor VIIIa light chain, particularly the A3 domain, and factor IXa (24). Further studies are warranted to clarify the precise interactions of protein S with factor VIIIa.

Acknowledgements

Abbreviations

VWF: von Willebrand factor, APC: activated protein C, wild-type A2: wt-A2, mAb: monoclonal antibody, EDC: 1-ethyl-3-(3-dimethylaminopropyl)-carbodiimide, SDS-PAGE: sodium dodecyl sulfate-polyacrylamide gel electrophoresis, HEPES: 4-(2-hydroxyethyl)-1-piperazineethanesulfonic acid, PBS: phosphate-buffered saline, HBS: Hepes-buffered saline, CAPS: 3-(cyclo-hexylamino)-1-propanesulfonic acid, SPR: surface plasmon resonance, ELISA: enzyme-linked immunosorbent assay, HSA: human serum albumin, PVDF: polyvinylidene difluoride, LRP: low-density lipoprotein receptor-related protein

References

1. Mann KG, Nesheim ME, Church WR, et al. Surface-dependent reactions of the vitamin K-dependent enzyme complexes. Blood 1990; 76: 1–16.
2. Wood WI, Capon DJ, Simonsen CC, et al. Expression of active human factor VIII from recombinant DNA clones. Nature 1984; 312: 330–337.
3. Vehar GA, Keyt B, Eaton D, et al. Structure of human factor VIII. Nature 1984; 312: 337–42.
4. Fay PJ, Anderson MT, Chavin SI, et al. The size of human factor VIII heterodimers and the effects produced by thrombin. Biochim Biophys Acta 1986; 871: 268–278.
5. Lollar P, Hill-Eubanks DC, Parker CG. Association of the factor VIII light chain with von Willebrand factor. J Biol Chem 1988; 263: 10451–10455.
6. Foster PA, Fulcher CA, Houghten RA, et al. An immunogenic region within residues Val1670-Glu1684 of the factor VIII light chain induces antibodies which inhibit binding of factor VIII to von Willebrand factor. J Biol Chem 1988; 263: 5230–5234.
7. Saenko EL, Shima M, Rajalakshmi KJ, et al. A role for the C2 domain of factor VIII in binding to von Willebrand factor. J Biol Chem 1994; 269: 11601–11605.
8. Eaton D, Rodriguez H, Vehar GA. Proteolytic processing of human factor VIII. Correlation of specific cleavages by thrombin, factor Xa, and activated protein C with activation and inactivation of factor VIII coagulant activity. Biochemistry 1986; 25: 505–512.
9. Fay PJ. Activation of factor VIII and mechanisms of cofactor action. Blood Rev 2004; 18: 1–15.
10. Fay PJ, Mastri M, Koszelak ME, et al. Cleavage of factor VIII heavy chain is required for the functional interaction of a2 subunit with factor IXa. J Biol Chem 2001; 276: 12434–12439.
11. Regan LM, Fay PJ. Cleavage of factor VIII light chain is required for maximal generation of factor VIIIa activity. J Biol Chem 1995; 270: 8546–8552.
12. Donath MS, Lenting PJ, van Mourik JA, et al. The role of cleavage of the light chain at positions Arg1689 or Arg1721 in subunit interaction and activation of

human blood coagulation factor VIII. J Biol Chem 1995; 270: 3648–3655.
13. Lamphear BJ, Fay PJ. Proteolytic interactions of factor IXa with human factor VIII and factor VIIIa. Blood 1992; 80: 3120–3126.
14. Nogami K, Shima M, Matsumoto T, et al. Mechanisms of plasmin-catalyzed inactivation of factor VIII: a crucial role for proteolytic cleavage at Arg336 responsible for plasmin-catalyzed factor VIII inactivation. J Biol Chem 2007; 282: 5287–5295.
15. DiScipio RG, Davie EW. Characterisation of protein S a gamma-carboxyglutamic acid containing protein from bovine and human plasma. Biochemistry 1979; 18: 899–904.
16. Walker FJ. Regulation of activated protein C by a new protein. A possible function for bovine protein S. J Biol Chem 1980; 255: 5521–5524.
17. Comp PC, Esmon CT. Recurrent venous thromboembolism in patients with a partial deficiency of protein S. N Engl J Med 1984; 311: 1525–1528.
18. Bertina RM. Hereditary protein S deficiency. Haemostasis 1985; 15: 241–246.
19. Heeb MJ, Mesters RM, Tans G, et al. Binding of protein S to factor Va associated with inhibition of prothrombinase that is independent of activated protein C. J Biol Chem 1993; 268: 2872–2832.
20. Heeb MJ, Rosing J, Bakker HN, et al. PS binds to and inhibits FXa. Proc. Natl. Acad. Sci. 1994; 91: 2728–2727.
21. Hackeng T, Sere KM, Tans G, et al. PS stimulates inhibition of the tissue factor pathway by TFPI. Proc. Natl. Acad. Sci. 2006; 103: 3106–3111.
22. Rosing J, Maurissen LFA, Tchaikovski SN, et al. Protein S is a cofactor for tissue factor pathway inhibitor. Thromb Res 2008; 122: (suppl 1) S60–63.
23. Koppelman SJ, Hackeng TM, Sixma JJ, et al. Inhibition of the intrinsic factor X activating complex by protein S: evidence for a specific binding of protein S to factor VIII. Blood 1995; 86: 1062–1071.
24. Takeyama M, Nogami K, Saenko EL, et al. Protein S down-regulates factor Xase activity independent of

activated protein C: specific binding of factor VIII(a) to protein S inhibits interactions with factor IXa. Br J Haematol 2008; 143: 409–420.
25. Bradford MM. A rapid and sensitive method for the quantitation of microgram quantities of protein utilizing the principle of protein-dye binding. Anal Biochem 1976; 72: 248–254.
26. Healey JF, Lubin I, Nakai H, et al. Residues 484–508 contain a major determinant of the inhibitory epitope in the A2 domain of human factor VIII. J Biol Chem 1995; 270: 14505–14509.
27. Sarafanov AG, Makogonenko EM, Pechik IV, et al. Identification of coagulation factor VIII A2 domain residues forming the binding epitope for low-density lipoprotein receptor-related protein. Biochemistry 2006; 45: 1829–1840.
28. Laemmli UK. Cleavage of structural proteins during the assembly of the head of bacteriophage T4. Nature 1970; 227: 680–685.
29. Fay PJ, Scandella D. Human inhibitor antibodies specific for the factor VIII A2 domain disrupt the interaction between the subunit and factor IXa. J Biol Chem 1999; 274: 29826–29830.
30. Nogami K, Lapan KA, Zhou Q, et al. Identification of a factor Xa-interactive site within residues 337–372 of the factor VIII heavy chain. J Biol Chem 2004; 279: 15763–15771.
31. Carraway KL, Koshland DE. Carbodiimide modification of proteins. Meth Enzym 1972; 25: 616–623.
32. O'Brien LM, Huggins CF, Fay PJ. Interacting regions in the A1 and A2 subunits of factor VIIIa identified by zero-length cross-linking. Blood 1997; 90: 3943–3950.
33. Nogami K, Nishiya K, Saenko EL, et al. Identification of a plasmin-interactive site within the A2 domain of the factor VIII heavy chain. Biochim Biophys Acta 2008; 1784: 753–763.
34. Nogami K, Saenko EL, Takeyama M, et al. Identification of a thrombin-interactive site within the FVIII A2 domain that is responsible for the cleavage at Arg372. Br J Haematol 2008; 140: 433–443.

35. Jenkins PV, Dill JL, Zhou Q, et al. Clustered basic residues within segment 484–510 of the factor VIIIa A2 subunit contribute to the catalytic efficiency for factor Xa generation. J Thromb Haemost. 2004; 2: 452–458.

36. Fay PJ, Beattie T, Huggins CF, et al. Factor VIIIa A2 subunit residues 558–565 represent a factor IXa interactive site. J Biol Chem 1994; 269: 20522– 20527.

37. Jenkins PV, Dill JL, Zhou Q, et al. Contribution of factor VIIIa A2 and A3-C1-C2 subunits to the affinity for factor IXa in factor Xase. Biochemistry 2004; 43: 5094–5101.

38. Fersht AR, Shi JP, Knill-Jones J, et al. Hydrogen bonding and biological specificity analysed by protein engineering. Nature 1985; 314: 235–238.

39. Pemberton S, Lindley P, Zaitsev V, et al. A molecular model for the triplicated A domains of human factor VIII based on the crystal structure of human ceruloplasmin. Blood 1997; 89: 2413–2421.

40. Church WR, Jernigan RL, Toole J, et al. Coagulation factors V and VIII and ceruloplasmin constitute a family of structurally related proteins. Proc Natl Acad Sci USA 1984; 81: 6934–6937.

41. Heeb MJ, Kojima Y, Hackeng TM, et al. Binding sites for blood coagulation factor Xa and protein S involving residues 493–506 in factor Va. Protein Sci 1996; 5: 1883–1889.

42. Fernández JA, Heeb MJ, Griffin JH. Identification of residues 413–433 of plasma protein S as essential for

binding to C4b-binding protein. J Biol Chem 1993; 268: 16788–16794.

43. Linse S, Härdig Y, Schultz DA, et al. A region of vitamin K-dependent protein S that binds to C4b binding protein (C4BP) identified using bacteriophage peptide display libraries. J Biol Chem 1997; 272: 14658–14665.

44. Heeb MJ, Kojima Y, Rosing J, et al. C-terminal residues 621–635 of protein S are essential for binding to factor Va. J Biol Chem 1999; 274: 36187–36192.

Identification of Plasmin-interactive Sites in the Light Chain of Factor VIII Responsible for Proteolytic Cleavage at Lys[36]*

Keiji Nogami[‡1], Katsumi Nishiya[‡], Evgueni L. Saenko[§], Masahiro Takeyama[‡], Kenichi Ogiwara[‡], Akira Yoshioka[‡], and Midori Shima[‡]

From the [‡]Department of Pediatrics, Nara Medical University, Kashihara, Nara 634-8522, Japan and the [§]Department of Biochemistry and Molecular Biology, University of Maryland School of Medicine, Baltimore, Maryland 21201

We have recently reported that plasmin likely associates with the factor VIII light chain to proteolyze at Lys[36] within the A1 domain. In this study, we determined that the rate of plasmin-catalyzed inactivation on the forms of factor VIIIa containing A1-(1–336) and [1722]A3C1C2, reflecting Lys[36] cleavage, was reduced by ~60%, compared with those containing [1649]A3C1C2 and [1690]A3C1C2. SDS-PAGE analysis revealed that Lys[36] cleavage of factor VIIIa with [1722]A3C1C2 was markedly slower than those with [1649]A3C1C2 and [1690]A3C1C2. Surface plasmon resonance-based assays, using active site-modified anhydro-plasmin (Ah-plasmin) showed that [1722]A3C1C2 bound to Ah-plasmin with an ~3-fold lower affinity than [1649]A3C1C2 or [1690]A3C1C2 (K_d, 176, 68.2, and 60.3 nM, respectively). Recombinant A3 bound to Ah-plasmin (K_d, 44.2 nM), whereas C2 failed to bind, confirming the presence of a plasmin-binding site within N terminus of A3. Furthermore, the Glu-Gly-Arg active site-modified factor IXa also blocked [1722]A3C1C2 binding to Ah-plasmin by ~95%, supporting the presence of another plasmin-binding site overlapping the factor IXa-binding site in A3. In keeping with a major contribution of the lysine-binding sites in plasmin for interaction with the factor VIII light chain, analysis of the A3 sequence revealed two regions involving clustered lysine residues in 1690–1705 and 1804–1818. Two peptides based on these regions blocked [1649]A3C1C2 binding to Ah-plasmin by ~60% and plasmin-catalyzed Lys[36] cleavage of factor VIIIa with A1-(1–336) by ~80%. Our findings indicate that an extended surface, centered on residues 1690–1705 and 1804–1818 within the A3 domain, contributes to a unique plasmin-interactive site that promotes plasmin docking during cofactor inactivation by cleavage at Lys[36].

Factor VIII circulates as a complex with von Willebrand factor and functions as an essential cofactor in the tenase complex responsible for anionic phospholipid surface-dependent conversion of factor X to Xa by factor IXa (1). Molecular defects in factor VIII result in the congenital bleeding disorder, hemo-

philia A. Factor VIII is composed of 2,332 amino acid residues with a molecular mass of ~300 kDa and contains three types of structural domain, arranged in the order of A1-A2-B-A3-C1-C2 (2, 3). Mature factor VIII is processed to a series of metal ion-dependent heterodimers by cleavage at the B-A3 junction, generating a heavy chain consisting of the A1 and A2 domains, together with heterogeneous fragments of a partially proteolyzed B domain, linked to a light chain consisting of the A3, C1, and C2 domains (2–4).

Factor VIII is converted into an active form, factor VIIIa, by limited proteolysis catalyzed by either thrombin or factor Xa (5). Cleavages at Arg[372] and Arg[740] in the heavy chain produce 50-kDa A1 and 40-kDa A2 subunits. Cleavage of the 80-kDa light chain ([1649]A3C1C2) at Arg[1689] produces a 70-kDa A3C1C2 subunit ([1690]A3C1C2). Additional cleavage by factor Xa at Arg[1721] produces a 67-kDa A3C1C2 subunit ([1722]A3C1C2). Proteolysis at Arg[372] and Arg[1689] is essential for generating factor VIIIa cofactor activity (6). Cleavage at the former site exposes a functional factor IXa-interactive site within the A2 domain that is cryptic in the unactivated molecule (7). Cleavage at the latter site liberates the cofactor from its carrier protein, von Willebrand factor (8), and contributes to the overall specific activity of the cofactor (9, 10).

APC[2] (5), factor Xa (5), and factor IXa (11) are serine proteases that inactivate factor VIII(a) by cleavage at Arg[336] within the A1 subunit. This inactivation appears to be associated with an altered interaction between the A2 subunit and truncated A1 and is coupled with an increase in the K_m value for the substrate, factor X (12, 13), reflecting loss of a factor X-interactive site within residues 337–372 (14). In addition, a second specific cleavage site for factor Xa, Lys[36], was identified within the A1 subunit (13). Attack at this site also results in factor VIII inactivation mediated by an altered conformation of the A1 subunit limiting productive interaction with the A2 subunit (13).

Plasmin is a potent fibrinolytic protease and is composed of a heavy chain consisting of five kringle domains and a light chain containing the catalytic domain. The protease associates with numerous proteins via the LBS on the exposed surface (15). Several reports have shown that plasmin proteolytically inacti-

2 The abbreviations used are: APC, activated protein C; LBS, lysine-binding site; EGR-factor IXa, Glu-Gly-Arg active site-modified factor IXa; mAb, monoclonal antibody; rA3, recombinant A3; rC2, recombinant C2; Ah-plasmin, anhydro-plasmin; CAPS, 3-(cyclohexylamino)-1-propanesulfonic acid; SPR-based assay, surface plasmon resonance-based assay; ELISA, enzyme-linked immunosorbent assay.

vates several coagulation proteins, including factors Va (16, 17), VIII (18), IXa (19), and X (20). In detail, we have demonstrated that plasmin rapidly inactivates factor VIII by cleavage at Arg[336] (18). Direct binding assays using Ah-plasmin, a catalytically inactive derivative of plasmin, revealed that plasmin interacts with the factor VIII heavy chain, predominantly the A2 domain, with high affinity (K_d, ~6 and ~20 nM, respectively), in a mechanism largely independent of LBS (21). Our findings demonstrated, in particular, that Arg[484] in the A2 domain significantly contributes to a unique plasmin-interactive site within the heavy chain that promotes plasmin docking during cleavage of the heavy chain (21).

In contrast, plasmin interacts with the factor VIII light chain with moderate affinity (K_d, ~70 nM), predominantly through LBS-dependent mechanisms (21). Our previous data suggested that plasmin cleavage at Lys[36] within the A1 domain appears to be selectively regulated by the light chain (18). In this study, we have expanded our studies using truncated light chain, recombinant factor VIII subunits, and synthetic peptides, and identified plasmin-interactive sites within the light chain responsible for cleavage at Lys[36]. Our results indicate that an extended surface centered on lysine residues involving the 1690–1705 and 1804–1818 regions in the A3 domain contributes to a unique plasmin-interactive site that promotes plasmin docking during cofactor inactivation by cleavage of the heavy chain at Lys[36].

MATERIALS AND METHODS

Reagents—Purified recombinant factor VIII preparations and the monoclonal antibody (mAb58.12) recognizing the N terminus of the A1 domain (22) were generous gifts from the Bayer Corp. (Osaka, Japan). The mAb NMC-VIII/5 recognizing the C2 domain was purified as described previously (23). Purified human plasmin (Lys-plasmin) devoid of factor Xa or APC was purchased from Sigma. Ah-plasmin, a catalytically inactive derivative of plasmin in which the active site serine is replaced by dehydroalanine, was prepared as described previously (21). The modified product demonstrated <1% plasmin activity, and its molecular weight was similar to that of native plasmin. Factor IXa, Glu-Gly-Arg active site-modified factor IXa (EGR-factor IXa), factor Xa, and thrombin were obtained from Hematologic Technologies Inc. (Essex Junction, VT). Pefabloc and horseradish peroxidase-labeled streptavidin were purchased from Roche Applied Science and Chemicon (Melbourne, Australia), respectively. Phospholipid vesicles containing 10% phosphatidylserine, 60% phosphatidylcholine, and 30% phosphatidylethanolamine (Sigma) were prepared using *N*-octyl glucoside (24). The mAb IgG preparations were biotinylated using *N*-hydroxysuccinimido-biotin reagent (Pierce). Synthetic peptides corresponding to factor VIII A3 residues 1690–1705 and 1804–1818 were prepared by BioSynthesis, Inc. (Lewisville, TX).

Isolation of Factor VIIIa Subunits—The intact light chain ([1649]A3C1C2) and heavy chain were isolated from factor VIII following the SP- and Q-Sepharose chromatography (Amersham Biosciences) (7). The [1690]A3C1C2 and [1722]A3C1C2 subunits were purified from thrombin- and factor Xa-cleaved [1649]A3C1C2 subunit, respectively, following SP-Sepharose chromatography (10, 25). The A1-(1–372) subunit was purified

from thrombin-cleaved heavy chain using Mono Q columns (12). The A1-(1–336) and A1-(37–336) subunits were purified from APC- and factor Xa-cleaved A1 subunits, following SP- and chelate-Sepharose, respectively (13). Factor VIIIa was isolated from thrombin-cleaved factor VIII by CM-Sepharose chromatography (Amersham Biosciences) (27). SDS-PAGE and staining of the isolated subunits with GelCode Blue Stain Regent (Pierce) showed >95% purity. Protein concentrations were determined by the method of Bradford (28).

Expression and Purification of Recombinant A3 (rA3) and C2 (rC2) Domains—The rA3 domain of factor VIII (residues 1690–2019) was expressed in *Escherichia coli* using the pET expression system (Novagen, Madison, WI). The pMT2/factor VIII plasmid containing the B domain-deleted factor VIII gene (29) was obtained from Dr. Pipe (University of Michigan, Ann Arbor, MI). DNA fragments encoding the A3 domain were generated by PCR using pMT2/factor VIII as a template and a pair of corresponding primers. The amplified fragments were ligated with pET-20b(+) expression vectors. Plasmid DNA was purified, and the sequence was confirmed by direct sequencing in both directions using Applied Biosystems technology (Foster City, CA). The plasmid was used for transformation of Origami(DE3)pLysS *E. coli* cells (Novagen), the host strain for the protein expression. The protein was expressed and subsequently purified using a His-Select affinity cartridge (Sigma). Proper folding of the rA3 fragment was confirmed by determination of the affinities for conformationally sensitive anti-A3 mAb CLB-CAgA (30). The cDNA coding the C2 domain sequence of human factor VIII was constructed, transformed into *Pichia pastoris* cells, and expressed in a yeast secretion system as described previously (31). The rC2 protein was purified by ammonium sulfate fractionation and CM-Sepharose chromatography (Amersham Biosciences) as described previously (31).

Reconstitution of Factor VIIIa Form—The A1/A3C1C2 dimer was reconstituted by mixing 500 nM of A1 form (A1-(1–372), A1-(1–336), and A1-(37–336)) and an equimolar amount of A3C1C2 form ([1649]A3C1C2, [1690]A3C1C2, and [1722]A3C1C2) overnight at 4 °C in 20 mM HEPES, pH 7.2, 0.3 M NaCl, 25 mM CaCl$_2$, and 0.01% Tween 20 (13). Furthermore, the reconstituted A1/A3C1C2 dimer forms (100 nM) were reacted with the excess amounts (300 nM) of A2 subunit for >15 min at 22 °C to minimize the A2 subunit dissociation from factor VIIIa. Reaction for >15 min generated the maximal factor VIIIa activity.

Factor Xa Generation Assay—The rate of conversion of factor X to factor Xa was monitored in a purified system (13). Plasmin-catalyzed inactivation of factor VIIIa was performed in HBS buffer (20 mM HEPES, pH 7.2, 0.1 M NaCl, 5 mM CaCl$_2$, 0.01% Tween 20) containing 0.1% bovine serum albumin and phospholipid vesicles (10 μM). Samples were removed from the mixtures at the indicated times, and plasmin reaction was immediately quenched by the addition of 0.2 mM Pefabloc and dilution. All reactions were performed at 37 °C. Factor Xa generation was initiated by the addition of factor IXa (20 nM) and factor X (400 nM) in the presence of phospholipid (10 μM). The reaction was quenched by addition of EDTA (100 mM). Rates of factor Xa generation were determined at 405 nm using a microtiter plate reader after the addition of chromogenic substrate,

S-2222 (0.46 mM final concentration). A control experiment showed that the presence of plasmin and Pefabloc in the diluted samples did not affect this assay (data not shown). Factor VIIIa activity was determined as the amount (in nanomoles) of factor Xa generated per min and converted into the amount (in nanomoles) of factor VIIIa.

Experiments assessing the stability of factor VIIIa were performed in the absence of plasmin to determine the rates of factor VIIIa activity loss resulting from the A2 dissociation. At the concentrations employed, ~5% loss of the initial activity was observed over a 20-min time course. Thus, for each time point in this experiment, including plasmin, the observed residual activity was corrected for the contribution of activity loss from the plasmin-independent mechanism.

Cleavage of Factor VIIIa Forms by Plasmin—Human plasmin (4 nM) was added to the reconstituted factor VIIIa forms (100 nM) at 37 °C in HBS buffer containing phospholipid vesicles (10 μM). Samples were obtained at the indicated times, and the reactions were immediately terminated and prepared for PAGE by adding SDS and 2-mercaptoethanol and boiling for 3 min.

Electrophoresis and Western Blotting—SDS-PAGE was performed using 8% gels by the procedure of Laemmli (32). Electrophoresis was carried out at 150 V for 1 h. For Western blotting, the proteins were transferred to a polyvinylidene difluoride membrane at 50 V for 2 h in buffer containing 10 mM CAPS, pH 11, and 10% (v/v) methanol. Proteins were probed using anti-A1 mAb58.12, followed by goat anti-mouse peroxidase-linked secondary antibody (MP Biomedicals, Aurora, OH). The signals were detected using the enhanced chemiluminescence system (PerkinElmer Life Sciences).

Kinetics Measurements Using Real Time Biomolecular Interaction Analysis—The kinetics of factor VIII light chain and plasmin interaction were determined by SPR-based assays using a BIAcore X instrument (BIAcore AB, Uppsala, Sweden) as reported previously (21). Ah-plasmin was covalently coupled (~7 ng/mm^2) to a CM5 sensor chip surface. Association of the ligand was monitored at a flow rate of 20 μl/min for 4 min. The dissociation of bound ligand was recorded over a 4-min period by replacing the ligand-containing buffer with buffer alone. The level of nonspecific binding corresponding to ligand binding to the uncoated chip was subtracted from the signal. The reactions were run at 37 °C. The rate constants for association (k_a) and dissociation (k_d) were determined by nonlinear regression analysis using the evaluation software provided by BIAcore AB. Equilibrium dissociation constants (K_d) were calculated as k_d/k_a.

ELISA Binding Assays Using Immobilized Ah-plasmin—These assays were performed as reported previously (21). Briefly, Ah-plasmin (200 nM) was coated onto microtiter wells overnight at 4 °C. The wells were blocked with 5% bovine serum albumin for 2 h at 37 °C, and various concentrations of the A3C1C2 subunits were added and incubated for 2 h at 37 °C. Biotinylated anti-C2 NMC-VIII/5 mAb IgG (1 μg) was added to each well, and bound IgG was detected by addition of horseradish peroxidase-labeled streptavidin. The absorbance was measured at 492 nm with a Labsystems Multiskan Multisoft microplate reader (Labsystems, Helsinki, Finland). The amount of nonspecific binding of biotinylated IgG, observed in the

absence of A3C1C2, was <5% of the total signal, and the amount of specific binding was obtained by subtracting the amount of nonspecific binding of biotinylated IgG.

Data Analysis—All experiments were performed at least three separate times. The parameters and their standard errors are shown. Nonlinear least squares or linear regression analysis was performed by KaleidaGraph (Synergy Reading, PA). The rates of the slope of first several points (within 5 min) in the time course of the plasmin-catalyzed inactivation of factor VIIIa form were fitted to a straight line from linear regression, and the obtained values were expressed as the inactivation rate. All correlation values (r) were >0.99.

Analyses of the interactions between the different forms of A3C1C2 and Ah-plasmin in ELISA were performed by a single-site binding model using Equation 1,

$$A = \frac{A_{max} \cdot [S]}{K_d + [S]} \qquad \text{(Eq. 1)}$$

where [S] is the concentration of A3C1C2 form in the solid-phase binding assay; K_d is the dissociation constant; and A_{max} represents maximum absorbance signal when the site is saturated by the A3C1C2 form.

Data from studies assessing the EGR-factor IXa or A3 synthetic peptide-dependent inhibition of plasmin interaction with A3C1C2 form were fitted by nonlinear least squares regression by using Equation 2,

$$\% \text{ binding} = \frac{B_{max} \cdot [\text{A3C1C2 form}]}{K_d \cdot \left(1 + \frac{[L]}{K_i}\right) + [\text{A3C1C2 form}]} + C$$

(Eq. 2)

where L represents the concentration of EGR-factor IXa or A3 peptide; B_{max} represents maximum binding; K_d is the dissociation constant for the interaction between the A3C1C2 form and Ah-plasmin; K_i is the apparent inhibition constant for L; and C is a constant for binding of the A3C1C2 form and Ah-plasmin that was unaffected by L.

RESULTS

Plasmin-catalyzed Inactivation of Factor VIIIa Reconstituted with the A1$^{1-336}$ and Various A3C1C2 Forms—We have recently reported that plasmin appears to associate with the light chain of factor VIII to regulate the proteolytic cleavage at Lys^{36} within the A1 subunit by its protease (18). To investigate whether the light chain contributes to plasmin-catalyzed factor VIIIa inactivation because of Lys^{36} cleavage, we first examined the effect on plasmin-catalyzed inactivation of factor VIIIa forms reconstituted with various A3C1C2 forms. Intact A1-(1–372) subunit is proteolyzed at Arg^{336} and Lys^{36} by plasmin, and the former cleavage significantly contributes to the factor VIIIa inactivation (18). Therefore, the A1-(1–336) subunit was utilized instead of the A1-(1–372) to observe the effect of Lys^{36} cleavage alone. Factor VIIIa forms were reconstituted in two-step procedures. The A1-(1–336)/A3C1C2 dimer forms were prepared by reacting the equimolar concentrations (500 nM) of the A1-(1–336) and isolated A3C1C2 subunits (^{1649}A3C1C2,
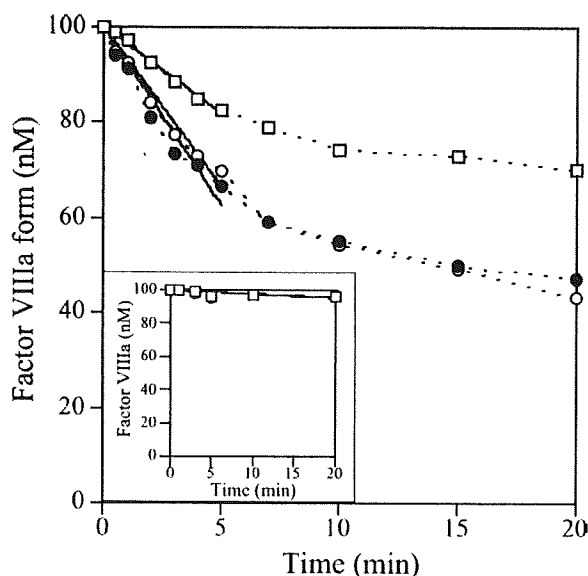
FIGURE 1. **Plasmin-catalyzed inactivation of factor VIIIa forms reconstituted with various A1 and A3C1C2 subunits.** The A1-(1–336) or A1-(37–336) (*inset*) subunit was reconstituted with the [1649]A3C1C2 (*open circles*), [1690]A3C1C2 (*closed circles*), and [1722]A3C1C2 (*open squares*) subunits as described under "Materials and Methods." The A1/A3C1C2 dimers (100 nM) were reacted with the A2 subunit (300 nM) and phospholipid vesicles (10 μM). Factor VIIIa inactivation was then monitored over time in the presence of plasmin (1 nM) using a factor Xa generation assay. Plasmin-catalyzed inactivation values were corrected by subtracting the corresponding values for factor VIIIa decay observed in the absence of plasmin. *Solid lines* were drawn from the linear regression fitting to evaluate the rate of plasmin-catalyzed inactivation of factor VIIIa with A1-(1–336) or A1-(37–336).

[1690]A3C1C2, and [1722]A3C1C2) in the presence of Ca^{2+}. The resultant dimers were diluted 5-fold and reacted with the A2 subunit (300 nM) to generate factor VIIIa heterotrimers. The A2 subunit was used at higher concentration to minimize its inactivation because of A2 dissociation from A1/A3C1C2 dimer. Inactivation of various factor VIIIa forms were then monitored over time in the presence of plasmin (1 nM) and phospholipid vesicles (10 μM) using a factor Xa generation assay as described under "Materials and Methods." The presence of plasmin and Pefabloc in the diluted samples did not affect this assay (data not shown). These data are illustrated in Fig. 1 and Table 1.

In the absence of plasmin, the maximal generated factor Xa obtained at saturable levels of reconstituted factor VIIIa with A1-(1–336) and the loss (decay) of its activity were similar (V_{max}, ~55 nM/min and ~5% activity loss at 20 min, respectively), independent of various A3C1C2 forms (data not shown). The activity of factor VIIIa forms with [1649]A3C1C2 subunit was rapidly reduced in a time-dependent manner by the addition of plasmin, similar to that of factor VIIIa with [1690]A3C1C2, with similar inactivation rates. The reduced activity reached ~55% of initial activity at 20 min. Of interest, slower inactivation of factor VIIIa with [1722]A3C1C2 by plasmin was observed, compared with [1649]A3C1C2 and [1690]A3C1C2. The activity was reduced by ~30% at 20 min, and the inactivation rate was ~45% that observed with [1649]A3C1C2 and [1690]A3C1C2. These results suggested that the N terminus of the

TABLE 1

Rates of plasmin-catalyzed inactivation of factor VIIIa forms reconstituted with various A1 and A3C1C2 forms

Inactivation of factor VIIIa forms was estimated by the rate obtained using the straight line fitting by the first several points (within 5 min) of the data shown in Fig. 1. Data points represent mean $\pm$ S.D. values of at least three separate experiments.

A3C1C2 form	A1 form	
	$A1^{1-336}$	$A1^{37-336}$
	Inactivation rates	
[1649]A3C1C2	7.8 $\pm$ 0.2	0.2 $\pm$ 0.04
[1690]A3C1C2	7.9 $\pm$ 0.4	0.2 $\pm$ 0.05
[1722]A3C1C2	3.4 $\pm$ 0.2	0.2 $\pm$ 0.03

light chain might be associated with plasmin-catalyzed inactivation of factor VIIIa with A1-(1–336) mediated by cleavage at Lys^{36}.

To further examine that inactivation of factor VIIIa with A1-(1–336) subunit by plasmin attributed to Lys^{36} cleavage, we repeated the same experiments using factor VIIIa forms reconstituted with the A1-(37–336) subunit, deleting the A1-(1–36). Factor VIIIa forms with the A1-(37–336), and various A3C1C2 subunits were reconstituted by the same approach. Independent of A3C1C2 forms, the maximally generated factor Xa and the activity loss (decay) of factor VIIIa forms were similar (V_{max}, ~25 nM/min and ~5% activity loss, respectively) in the absence of plasmin (data not shown). Three factor VIIIa forms with A1-(37–336) were, however, little inactivated (by ~5%) by plasmin even at over a 20-min reaction (Fig. 1, *inset*). Inactivation rates were similar, supporting the view that plasmin-catalyzed inactivation of factor VIIIa with A1-(1–336) subunit was regulated by Lys^{36} cleavage.

Addition of Various A3C1C2 Forms on Plasmin-catalyzed Inactivation of Factor VIIIa with A1$^{1-336}$—To confirm that the N terminus of the A3C1C2 domain is responsible for plasmin-catalyzed inactivation of factor VIIIa, we examined the inhibitory effects by the addition of various A3C1C2 forms on these reactions. The A1-(1–336)/[1649]A3C1C2 dimer was reconstituted with excess amounts of A2 subunit, and factor VIIIa inactivation was then monitored by the addition of plasmin (1 nM) in the presence of various A3C1C2 in a factor Xa generation assay as described under "Materials and Methods." The presence of competitors, A3C1C2 forms, did not affect this assay (data not shown). These data are illustrated in Fig. 2 and Table 2. The addition of the [1649]A3C1C2 and [1690]A3C1C2 subunits, rA3 domain (residues 1690–2019) (75 nM), each similarly inhibited plasmin-catalyzed inactivation of factor VIIIa with A1-(1–336), with an ~55% decrease in inactivation rate. Furthermore, the addition of a higher concentration (250 nM) of these A3C1C2 forms showed ~90% decreases in inactivation rates. In contrast, in the presence of [1722]A3C1C2, the inactivation rates were reduced by ~30 and ~55% at both concentrations, respectively, and the inhibitory effects were less than those of the other three A3C1C2 forms. The presence of rC2 domain (residues 2174–2332) had little effect. Taken together, these findings indicated that the 1690–1721 region in the A3 domain contributed to plasmin-catalyzed inactivation of factor VIIIa through Lys^{36} cleavage.

Effects of the A3C1C2 Forms on Plasmin-catalyzed Cleavage at Lys^{36} within the A1 Domain—To evaluate visually the effect of the various A3C1C2 forms on cleavage by plasmin at Lys^{36} in